MATHEMATICS OF COMPUTATION
Volume 87, Number 310, March 2018, Pages 659–692
http://dx.doi.org/10.1090/mcom/3254
Article electronically published on June 21, 2017

BDDC ALGORITHMS WITH DELUXE SCALING AND ADAPTIVE SELECTION OF PRIMAL CONSTRAINTS FOR RAVIART-THOMAS VECTOR FIELDS

DUK-SOON OH, OLOF B. WIDLUND, STEFANO ZAMPINI, AND CLARK R. DOHRMANN

Abstract. A BDDC domain decomposition preconditioner is defined by a coarse component, expressed in terms of primal constraints, a weighted average across the interface between the subdomains, and local components given in terms of solvers of local subdomain problems. BDDC methods for vector field problems discretized with Raviart-Thomas finite elements are introduced. The methods are based on a deluxe type of weighted average and an adaptive selection of primal constraints developed to deal with coefficients with high contrast even inside individual subdomains. For problems with very many subdomains, a third level of the preconditioner is introduced.

Under the assumption that the subdomains are all built from elements of a coarse triangulation of the given domain, that the meshes of each subdomain are quasi uniform and that the material parameters are constant in each subdomain, a bound is obtained for the condition number of the preconditioned linear system which is independent of the values and the jumps of these parameters across the interface between the subdomains as well as the number of subdomains. Numerical experiments, using the PETSc library, are also presented which support the theory and show the effectiveness of the algorithms even for problems not covered by the theory. Included are also experiments with Brezzi-Douglas-Marini finite element approximations.

1. Introduction

Let Ω be a bounded Lipschitz domain in $\mathbb{R}^3$. We will work with the Hilbert space $H(\mathrm{div};\Omega)$, which is the subspace of vector valued functions $\boldsymbol{u} \in (L^2(\Omega))^3$ with $\mathrm{div}\,\boldsymbol{u} \in L^2(\Omega)$. The space $H_0(\mathrm{div};\Omega)$ is the subspace of $H(\mathrm{div};\Omega)$ with a vanishing normal component on the boundary $\partial\Omega$.

We will consider the following problem: Find $\boldsymbol{u} \in H_0(\mathrm{div};\Omega)$ such that

$$a(\boldsymbol{u},\boldsymbol{v}) := \int_\Omega (\alpha\,\mathrm{div}\,\boldsymbol{u}\,\mathrm{div}\,\boldsymbol{v} + \beta\,\boldsymbol{u}\cdot\boldsymbol{v})dx = \int_\Omega \boldsymbol{f}\cdot\boldsymbol{v}\,dx, \quad \forall \boldsymbol{v} \in H_0(\mathrm{div};\Omega). \tag{1.1}$$

We will assume that the coefficient α is a bounded, nonnegative function, that β is a strictly positive, bounded function, and that the right-hand side $\boldsymbol{f} \in (L^2(\Omega))^3$. We note that the norm of $\boldsymbol{u} \in H(\mathrm{div};\Omega)$ for a domain with a unit diameter is given by $(a(\boldsymbol{u},\boldsymbol{u}))^{1/2}$ with $\alpha = 1$ and $\beta = 1$.

The bilinear form (1.1) arises from the boundary value problem:

$$\begin{aligned} L\boldsymbol{u} := -\mathbf{grad}\,(\alpha\,\mathrm{div}\,\boldsymbol{u}) + \beta\,\boldsymbol{u} &= \boldsymbol{f} \text{ in } \Omega, \\ \boldsymbol{u}\cdot\boldsymbol{n} &= 0 \text{ on } \partial\Omega. \end{aligned} \tag{1.2}$$

Received by the editor January 18, 2016 and, in revised form, October 7, 2016.
2010 *Mathematics Subject Classification.* Primary 65F08, 65F10, 65N30, 65N55.
Key words and phrases. Domain decomposition, BDDC preconditioner, Raviart-Thomas finite elements, multilevel preconditioners, adaptive selection of coarse spaces.

Here, $\boldsymbol{n}$ is the outward unit normal vector of $\partial\Omega$. The boundary value problem (1.2) is equivalent to a mixed formulation of a first order system least-squares problem as in [17]. There are also other applications related to the $H(\mathrm{div})$ space, e.g., in iterative solvers for the Reissner-Mindlin plate, the sequential regularization method for the Navier-Stokes equations, and, possibly most importantly, mixed formulations of flow in porous media or Brinkman equations. For more details, see [6, 7, 51, 82].

Domain decomposition methods of iterative substructuring type for solving large linear algebraic systems originating from elliptic partial differential equations have been studied extensively; see [75]. Among these methods, the balancing Neumann-Neumann (BNN) and the finite element tearing and interconnecting (FETI) algorithms have proven quite successful; see, e.g., [28, 30, 31, 46, 54]. The balancing domain decomposition by constraints (BDDC) methods, introduced in [21], are modified BNN methods with a global component of the preconditioner determined by a set of primal continuity constraints between the subdomains. For a pioneering analysis for scalar elliptic problems, see [55, 56].

The BDDC methods are closely related to the dual-primal FETI (FETI-DP) methods [29, 59] as are the earlier BNN methods to the one-level FETI methods; see [32]. Thus, the spectra relevant to the performance of a BDDC and a FETI-DP algorithm will be the same, except possibly for eigenvalues of 0 and 1, for the same set of primal constraints; see [15, 50, 56]. Hence, we can use results for BDDC methods to obtain results for FETI-DP methods and vice versa.

The main purpose of this paper is to construct and analyze a BDDC preconditioner for vector field problems discretized with Raviart-Thomas finite elements. Iterative substructuring methods for Raviart-Thomas problems were first considered in [85] and we will use several auxiliary results from that study in the analysis of our method. BNN, FETI, and FETI-DP methods for these problems were developed in [71, 73, 74]. Overlapping Schwarz methods have also been introduced for vector field problems; see [7, 33, 62, 63, 72]. Other methods such as multigrid methods have been applied successfully in [8, 36, 44]. A multilevel preconditioner based on additive Schur complement approximations has been introduced in [45]; that paper is primarily focused on cases with very irregular coefficients.

BDDC methods have also been widely extended to other problems such as flow in porous media in [76, 77], incompressible Stokes equations in [49], Reissner-Mindlin plate models in [10, 47], advection-diffusion problems in [81], and Helmholtz equations in [48]. Multilevel BDDC methods were introduced in [21, 70, 78–80] and other discretization methods, e.g., spectral element methods and discontinuous Galerkin methods, have been considered in [27, 65, 66]. Recently, there has also been pioneering work on isogeometric element problems; see [11–13]. We will explore the use of three-level BDDC, which was first successfully studied in [78–80] for other elliptic problems. We note that the third author recently has written a series of papers on solving very large problems using BDDC and contributing to the PETSc library; cf. [86–90].

In the construction of a BDDC preconditioner, a set of primal constraints and a weighted averaging technique have to be chosen and these choices will very directly affect the rate of convergence. Effective primal constraints are very simple to find for the Raviart-Thomas elements; we primarily need a *no-net-flux* condition across each subdomain boundary. However, for problems with coefficients with large contrast, additional primal constraints are sometimes very useful. We will adaptively select

the primal constraints to deal with such coefficients as pioneered in [23, 67]. For recent work in this field, see also [20,38–40,57,58]. A unified framework has recently been developed in [68].

The choice of averaging proves to be intricate. We will use a recently developed type of weighted averaging technique, called *deluxe scaling*, introduced in [25] for three-dimensional $H(\mathbf{curl})$ problems. The deluxe scaling technique allows us to reduce the analysis to individual subdomains. Hence, a finite element extension theorem, which is needed in the analysis of other averaging techniques as in [42], is no longer needed.

In several previous studies on domain decomposition methods for vector field problems, [71, 73, 74, 85], the bound on the condition number of the preconditioned linear system depends on the ratio of the coefficients α and βH^2 where H is the diameter of the subdomain. Such results have been developed for a BDDC algorithm for three-dimensional problems in $H(\mathbf{curl})$; see [25] as well as [73]. This limitation has been removed in several recent studies. Among them is a paper on an iterative substructuring method for two-dimensional problems posed in $H(\mathbf{curl})$; see [24]. In more recent work results have been obtained for BDDC deluxe and overlapping Schwarz algorithms, again for two-dimensional problems posed in $H(\mathbf{curl})$; see [18, 19]. An overlapping Schwarz method for three-dimensional $H(\mathrm{div})$ problems has also been developed; see [63]. In that work, two sets of inequalities were developed to handle the mass-dominated and the divergence-dominated cases, respectively.

We know of no previous full analysis of BDDC or FETI-DP type methods for three-dimensional $H(\mathrm{div})$ problems; see [64] for an announcement of some of our results. We are able to provide BDDC methods with an upper bound on the condition number, which is independent of the values and the jumps of the coefficients across the interface and to obtain condition number bounds which are polylogarithmic in the number of degrees of freedom of the individual subdomains or only depend on a tolerance parameter used for an adaptive selection of primal constraints. While we are developing and testing our algorithms for quite general subdomains and material parameters, our proofs are restricted to subdomains which are convex and each a union of a finite number of coarse elements, with material parameters constant in each subdomain. When developing our theory, we also assume that the finite element triangulation of each subdomain is quasi-uniform.

The rest of this paper is organized as follows. In section 2, we introduce some standard Sobolev spaces, a finite element approximation based on Raviart-Thomas elements, and decompositions of the interface spaces. We introduce our BDDC algorithms for an interface problem and define various operators used to describe the algorithms in section 3; in its last subsection, we introduce adaptive three-level BDDC. We next provide some auxiliary results and a proof of our main result in section 4. Finally, section 5 contains results of numerical experiments, which extend our findings to irregular subdomains obtained by mesh partitioners and to higher order Raviart-Thomas elements and Brezzi-Douglas-Marini (BDM) elements; cf. [16].

2. Function and finite element spaces

2.1. **Continuous spaces.** We will use the Sobolev spaces $H^1(\Omega)$ and its trace space $H^{1/2}(\partial\Omega)$, equipped with their norms and semi-norms for bounded domains. The domain Ω and the subdomains, into which it is partitioned, are assumed to be

Lipschitz. Let H be the diameter of Ω. Then,

$$\|u\|^2_{1;\Omega} := |u|^2_{1;\Omega} + \frac{1}{H^2}\|u\|^2_{0;\Omega}, \qquad \|u\|^2_{1/2;\partial\Omega} := |u|^2_{1/2;\partial\Omega} + \frac{1}{H}\|u\|^2_{0;\partial\Omega},$$

where the L^2-norm $\|\cdot\|_{0;\Omega}$ and the semi-norms $|\cdot|_{1;\Omega}$ and $|\cdot|_{1/2;\partial\Omega}$ are defined by $\|u\|^2_{0;\Omega} := \int_\Omega |u|^2\, dx$, $|u|^2_{1;\Omega} := \int_\Omega |\nabla u|^2\, dx$, and

$$|u|^2_{1/2;\partial\Omega} := \int_{\partial\Omega}\int_{\partial\Omega} \frac{|u(x)-u(y)|^2}{|x-y|^3}\, dxdy,$$

respectively. The weights for the L^2-terms result from the standard definitions of the norms for a domain of diameter 1 and a dilation. We can also easily extend these definitions to vector-valued cases.

The space $H(\mathrm{div}\,;\Omega)$ is defined by

$$H(\mathrm{div}\,;\Omega) := \{\boldsymbol{u} \in (L^2(\Omega))^3 \,|\, \mathrm{div}\,\boldsymbol{u} \in L^2(\Omega)\}$$

with the scaled graph norm:

$$\|\boldsymbol{u}\|^2_{\mathrm{div};\Omega} := \|\mathrm{div}\,\boldsymbol{u}\|^2_{0;\Omega} + \frac{1}{H^2}\|\boldsymbol{u}\|^2_{0;\Omega}.$$

The normal component on the boundary $\partial\Omega$ of any $\boldsymbol{u} \in H(\mathrm{div};\Omega)$ belongs to $H^{-1/2}(\partial\Omega)$; see [16, 60]. The norm for the space $H^{-1/2}(\partial\Omega)$ is given by

$$\|\boldsymbol{u}\cdot\boldsymbol{n}\|_{-1/2;\partial\Omega} := \sup_{\phi\in H^{1/2}(\partial\Omega),\phi\neq 0} \frac{\langle \boldsymbol{u}\cdot\boldsymbol{n}, \phi\rangle}{\|\phi\|_{1/2;\partial\Omega}},$$

where the angle brackets stand for the duality product of $H^{-1/2}(\partial\Omega)$ and $H^{1/2}(\partial\Omega)$. We have the following trace theorem.

Lemma 2.1. *There exists a constant C, which is independent of the diameter of Ω, such that, for all $\boldsymbol{u} \in H(\mathrm{div};\Omega)$,*

$$\|\boldsymbol{u}\cdot\boldsymbol{n}\|^2_{-1/2;\partial\Omega} \le C(H^2\|\mathrm{div}\,\boldsymbol{u}\|^2_{0;\Omega} + \|\boldsymbol{u}\|^2_{0;\Omega}).$$

Proof. This follows directly from Green's formula on a domain of unit diameter and by applying a dilation; see [85, Lemma 2.1]. □

In developing our theory, we also need to work with the $H(\mathbf{curl}\,;\Omega)$ space defined by

$$H(\mathbf{curl}\,;\Omega) := \{\boldsymbol{u} \in (L^2(\Omega))^3 \,|\, \mathbf{curl}\,\boldsymbol{u} \in (L^2(\Omega))^3\}$$

with the scaled graph norm:

$$\|\boldsymbol{u}\|^2_{\mathbf{curl};\Omega} := \|\mathbf{curl}\,\boldsymbol{u}\|^2_{0;\Omega} + \frac{1}{H^2}\|\boldsymbol{u}\|^2_{0;\Omega}.$$

We finally introduce $H^1_0(\Omega)$, $H_0(\mathrm{div}\,;\Omega)$, and $H_0(\mathbf{curl}\,;\Omega)$ as the subspaces of $H^1(\Omega)$, $H(\mathrm{div}\,;\Omega)$, and $H(\mathbf{curl}\,;\Omega)$ with a vanishing boundary value, a vanishing normal component, and a vanishing tangential component on $\partial\Omega$, respectively.

2.2. **Finite element spaces.** In this paper, we will develop our theory for tetrahedral elements but we note that our results are equally valid for hexahedral elements. We remark that there are many useful tools, developed for hexahedral elements in [85], that can easily be modified for tetrahedral elements.

We first introduce a triangulation $\mathcal{T}_h$ of Ω into tetrahedral elements. We then decompose the domain Ω into N nonoverlapping subdomains Ω_i of diameter H_i. We assume that each subdomain Ω_i is a union of elements of the triangulation $\mathcal{T}_h$ and that each Ω_i is simply connected and has a connected boundary. We also assume that the triangulation $\mathcal{T}_h$ is shape regular with nodes matching across the interface between the subdomains and, when developing our theory, that the triangulation is quasi-uniform on each subdomain. The smallest diameter of the elements of Ω_i is denoted by h_i. In our estimates, we will use the fraction H/h to denote

$$H/h := \max_{1\leq i\leq N} \{H_i/h_i\}.$$

We also define the interface Γ by

$$\Gamma := \left(\bigcup_{i=0}^{N} \partial\Omega_i\right) \backslash \partial\Omega$$

and the local interfaces Γ_i by

$$\Gamma_i := \Gamma \cap \partial\Omega_i.$$

For our analysis, we will consider the lowest order Raviart-Thomas elements on the mesh $\mathcal{T}_h$; see [16, Chapter 3] and [61]. The Raviart-Thomas elements are conforming in $H(\mathrm{div}\,;\Omega)$ and those of lowest order are defined by

$$W(\Omega) := \{\boldsymbol{u} \mid \boldsymbol{u}_{|K} \in \mathcal{RT}(K), K \in \mathcal{T}_h \text{ and } \boldsymbol{u} \in H(\mathrm{div}\,;\Omega)\},$$

where the shape function $\mathcal{RT}(K)$ is given by four scalar parameters

$$\mathcal{RT}(K) := \begin{pmatrix} a_1 \\ a_2 \\ a_3 \end{pmatrix} + b \begin{pmatrix} x \\ y \\ z \end{pmatrix}$$

for a tetrahedral element. The degrees of freedom for an element K in $\mathcal{T}_h$ are given by

$$\lambda_f(\boldsymbol{u}) := \frac{1}{|f|} \int_f \boldsymbol{u} \cdot \boldsymbol{n}\, ds, \qquad f \subset \partial K,$$

i.e., the average values of the normal components over the faces of the element. These four values determine a_1, a_2, a_3, and b. A basis function of the lowest order Raviart-Thomas element space is supported in two elements of $\mathcal{T}_h$, with the value of the normal component on a face equal to 1 for one of the elements and -1 for the other, while vanishing on all other faces. While our analysis will be limited to the lowest order Raviart-Thomas elements, we will consider higher order Raviart-Thomas elements and BDM elements in our experiments; such elements have additional degrees of freedom corresponding to moments of the normal component over element faces as well as degrees of freedom related with moments over element volume. For details, see [16].

The l^2-norm of the vector of the coefficients $\lambda_f(\boldsymbol{u})$ can be used to estimate the L^2-norm of $\boldsymbol{u}$ and of its divergence; the proof of the following lemma is elementary and a simple modification of [69, Proposition 6.3.1]. See also [85, Lemma 3.1].

Lemma 2.2. *Let $K \in \mathcal{T}_h$. Then, there exist strictly positive constants, c and C, depending only on the aspect ratio of K, such that for all $\boldsymbol{u} \in W$,*

$$c \sum_{f \subset \partial K} h_f^3 \lambda_f(\boldsymbol{u})^2 \leq \|\boldsymbol{u}\|_{0;K}^2 \leq C \sum_{f \subset \partial K} h_f^3 \lambda_f(\boldsymbol{u})^2$$

and

$$\|\operatorname{div} \boldsymbol{u}\|_{0;K}^2 \leq C \sum_{f \subset \partial K} h_f \lambda_f(\boldsymbol{u})^2,$$

where h_f is the diameter of f.

The following lemma follows directly from Lemma 2.2.

Lemma 2.3 (Inverse inequality)**.** *Let $K \in \mathcal{T}_h$. Then, there exists a constant C, depending only on the aspect ratio of K, such that for all $\boldsymbol{u} \in W$,*

$$h_K \|\operatorname{div} \boldsymbol{u}\|_{0;K} \leq C \|\boldsymbol{u}\|_{0;K}, \tag{2.1}$$

where h_K is the diameter of K.

We also need $\widehat{W}_0$, a finite element subspace of $H_0(\operatorname{div};\Omega)$:

$$\widehat{W}_0(\Omega) := W(\Omega) \cap H_0(\operatorname{div};\Omega).$$

We will now consider the variational problem (1.1). We obtain the stiffness matrix A by restricting this problem to $\widehat{W}_0$; A is symmetric and positive definite.

When developing our theory, we will need several additional spaces. Let S be the space of continuous, piecewise linear functions on the tetrahedral elements, and let S_0 be the subspace of elements of S which vanish on $\partial\Omega$. Let Q be the space of piecewise constant functions on the same elements. Finally, let X be the space of the lowest order Nédélec elements. We recall that the Lagrange P_1, Raviart-Thomas, and Nédélec spaces are conforming finite element spaces in H^1, $H(\operatorname{div})$, and $H(\mathbf{curl})$, respectively.

Let $\mathcal{V}_h$ and $\mathcal{F}_h$ be the set of vertices and faces of $\mathcal{T}_h$, respectively. The interpolation operators I_h, and ρ_h^{RT} for sufficiently smooth functions $u \in H^1$ and $\boldsymbol{v} \in H(\operatorname{div})$ onto S and W, respectively, are defined as follows:

$$I_h u := \sum_{p \in \mathcal{V}_h} u(p) \phi_p^P \quad \text{and} \quad \rho_h^{RT} \boldsymbol{v} := \sum_{f \in \mathcal{F}_h} \lambda_f(\boldsymbol{v}) \boldsymbol{\phi}_f^{RT},$$

where ϕ_p^P and $\boldsymbol{\phi}_f^{RT}$ are the basis functions of the P_1 and Raviart-Thomas spaces associated with the node p and the element face f, respectively. We also denote by Π_h the L^2-projection operator onto Q.

We finally recall the following error estimate for the Raviart-Thomas interpolation operator and a commuting property.

Lemma 2.4. *For any $\boldsymbol{u} \in (H^1(\Omega_i))^3$, we have*

$$\left\|\boldsymbol{u} - \rho_h^{RT} \boldsymbol{u}\right\|_{0;\Omega_i} \leq C h_i |\boldsymbol{u}|_{1;\Omega_i}.$$

Proof. See [14, Lemma 5.5]. □

Lemma 2.5. *For any $\boldsymbol{u} \in (S(\Omega_i))^3$, we have*

$$\left\|\rho_h^{RT} \boldsymbol{u}\right\|_{0;\Omega_i} \leq C \|\boldsymbol{u}\|_{0;\Omega_i}.$$

Proof. By using the triangle inequality, Lemma 2.4, and an inverse estimate for P_1 functions, we obtain

$$\begin{aligned}\left\|\rho_h^{RT}(\boldsymbol{u})\right\|_{0;\Omega_i}^2 &\le 2\left\|\boldsymbol{u}\right\|_{0;\Omega_i}^2 + 2\left\|\boldsymbol{u}-\rho_h^{RT}\boldsymbol{u}\right\|_{0;\Omega_i}^2 \\ &\le 2\left\|\boldsymbol{u}\right\|_{0;\Omega_i}^2 + Ch_i^2\left|\boldsymbol{u}\right|_{1;\Omega_i}^2 \le C\left\|\boldsymbol{u}\right\|_{0;\Omega_i}^2.\end{aligned} \tag{2.2}$$

□

Lemma 2.6. *Let $\boldsymbol{u}$ be sufficiently regular. Then, the following commuting property holds:*

$$\operatorname{div}\left(\rho_h^{RT}\boldsymbol{u}\right) = \Pi_h\left(\operatorname{div}\boldsymbol{u}\right). \tag{2.3}$$

Proof. See [14, Property 5.3]. □

We note that property (2.3) is a part of the discrete de Rham diagram described, e.g., in [60, section 5.7].

3. The BDDC methods

3.1. **The discrete problem.** The description of the BDDC algorithm and its analysis require the introduction of several spaces. Let $W^{(i)}$ be the space of the lowest order Raviart-Thomas finite elements on Ω_i with a zero normal component on $\partial\Omega\cap\partial\Omega_i$. We will decompose $W^{(i)}$ into two subspaces, an interior space $W_I^{(i)}$ and an interface space $W_\Gamma^{(i)}$. The interface space $W_\Gamma^{(i)}$ will then be decomposed into a primal space $W_\Pi^{(i)}$ and a dual space $W_\Delta^{(i)}$. Hence, we will have the following decompositions:

$$W^{(i)} := W_I^{(i)} \oplus W_\Gamma^{(i)} := W_I^{(i)} \oplus W_\Delta^{(i)} \oplus W_\Pi^{(i)}.$$

We will also use the following product spaces:

$$W_0 := \prod_{i=1}^N W^{(i)},\ W_I := \prod_{i=1}^N W_I^{(i)},\ W_\Gamma := \prod_{i=1}^N W_\Gamma^{(i)}$$

and

$$W_\Delta := \prod_{i=1}^N W_\Delta^{(i)},\ W_\Pi := \prod_{i=1}^N W_\Pi^{(i)}.$$

We then have

$$W_0 = W_I \oplus W_\Gamma = W_I \oplus W_\Delta \oplus W_\Pi.$$

The functions in W_Γ can have discontinuous normal components across the interface while those of the finite element solutions are continuous; the subspace with continuous normal components will be denoted by $\widehat{W}_\Gamma$. We also consider a space $\widetilde{W}_\Gamma$ of functions in the primal subspace having continuous normal components across the interface while those in the dual subspace potentially are discontinuous. We can then decompose $\widehat{W}_\Gamma$ and $\widetilde{W}_\Gamma$ into $\widehat{W}_\Delta \oplus \widehat{W}_\Pi$ and $W_\Delta \oplus \widehat{W}_\Pi$, respectively, where $\widehat{W}_\Delta$ is the continuous dual variable subspace and $\widehat{W}_\Pi$ is the continuous primal variable subspace.

We can now obtain the local stiffness matrix $A^{(i)}$ by restricting the bilinear form to Ω_i, i.e.,

$$a_i(\boldsymbol{u},\boldsymbol{v}) := \int_{\Omega_i} (\alpha \operatorname{div}\boldsymbol{u}\operatorname{div}\boldsymbol{v} + \beta\,\boldsymbol{u}\cdot\boldsymbol{v})dx, \tag{3.1}$$

and replacing $H(\mathrm{div};\Omega_i)$ by the finite element space $W^{(i)}$. It is convenient to make a change of variables by introducing a basis for the primal degrees of freedom and a complementary basis for the dual subspace $W_\Delta^{(i)}$ since the presentation of the algorithms and the theoretical results are considerably simplified using the new basis. Here we can follow the recipes of [50, subsection 3.3] closely. We note that there is also some evidence that such a change of variables enhances the numerical stability of BDDC and FETI-DP algorithms; see [41]. However, the change of variables can come with a loss of sparsity and there are alternative ways of implementing these algorithms; cf. [21].

After this change of variables, we find that the contributions from the subdomain Ω_i to the stiffness matrix and to the load vector can be written as

$$\begin{bmatrix} A_{II}^{(i)} & A_{I\Delta}^{(i)} & A_{I\Pi}^{(i)} \\ A_{I\Delta}^{(i)T} & A_{\Delta\Delta}^{(i)} & A_{\Delta\Pi}^{(i)} \\ A_{I\Pi}^{(i)T} & A_{\Delta\Pi}^{(i)T} & A_{\Pi\Pi}^{(i)} \end{bmatrix} \text{ and } \begin{bmatrix} \boldsymbol{f}_I^{(i)} \\ \boldsymbol{f}_\Delta^{(i)} \\ \boldsymbol{f}_\Pi^{(i)} \end{bmatrix}.$$

We then obtain the global linear system of algebraic equations by sub-assembling these local contributions:

$$A \begin{bmatrix} \boldsymbol{u}_I \\ \boldsymbol{u}_\Delta \\ \boldsymbol{u}_\Pi \end{bmatrix} = \begin{bmatrix} A_{II} & A_{I\Delta} & A_{I\Pi} \\ A_{I\Delta}^T & A_{\Delta\Delta} & A_{\Delta\Pi} \\ A_{I\Pi}^T & A_{\Delta\Pi}^T & A_{\Pi\Pi} \end{bmatrix} \begin{bmatrix} \boldsymbol{u}_I \\ \boldsymbol{u}_\Delta \\ \boldsymbol{u}_\Pi \end{bmatrix} = \begin{bmatrix} \boldsymbol{f}_I \\ \boldsymbol{f}_\Delta \\ \boldsymbol{f}_\Pi \end{bmatrix}, \tag{3.2}$$

where $\boldsymbol{u}_I \in W_I$, $\boldsymbol{u}_\Delta \in \widehat{W}_\Delta$, and $\boldsymbol{u}_\Pi \in \widehat{W}_\Pi$.

3.2. **Some useful operators.** We will now define several operators, most of which were introduced in [50], which perform restrictions, extensions, scalings, averaging, or imbeddings between different spaces. We first consider the restriction operators. $R_\Gamma^{(i)}$ maps the space $\widehat{W}_\Gamma$ to the subdomain subspace $W_\Gamma^{(i)}$. Similarly, we can define $\overline{R}_\Gamma^{(i)} : \widetilde{W}_\Gamma \to W_\Gamma^{(i)}$. Moreover, $R_\Delta^{(i)} : W_\Delta \to W_\Delta^{(i)}$ and $R_\Pi^{(i)} : \widehat{W}_\Pi \to W_\Pi^{(i)}$ map global interface vectors defined on Γ to their components on Γ_i. $\widetilde{R}_{\Gamma\Delta}$ and $\widetilde{R}_{\Gamma\Pi}$ are the restriction operators from the intermediate space $\widetilde{W}_\Gamma$ to W_Δ and $\widehat{W}_\Pi$, respectively. Similarly, we can define the restriction operator $R_{\Gamma\Delta}^{(i)}$ from $W_\Gamma^{(i)}$ to $W_\Delta^{(i)}$. R_Γ and $\overline{R}_\Gamma$ are the direct sums of all the $R_\Gamma^{(i)}$ and $\overline{R}_\Gamma^{(i)}$, respectively. Furthermore, the imbedding $\widetilde{R}_\Gamma : \widehat{W}_\Gamma \to \widetilde{W}_\Gamma$ is the direct sum of $\widehat{R}_\Pi$ and all the $\widehat{R}_\Delta^{(i)}$, where $\widehat{R}_\Pi$ represents the restriction from $\widehat{W}_\Gamma$ to $\widehat{W}_\Pi$ and $\widehat{R}_\Delta^{(i)}$ maps the space $\widehat{W}_\Gamma$ into $W_\Delta^{(i)}$.

We next introduce scaling matrices, $D^{(i)}$, acting on the degrees of freedom associated with the Γ_i. They are combined into a block diagonal matrix and should provide a discrete partition of unity, i.e.,

$$R_\Gamma^T \begin{bmatrix} D^{(1)} & & & \\ & D^{(2)} & & \\ & & \ddots & \\ & & & D^{(N)} \end{bmatrix} R_\Gamma = I. \tag{3.3}$$

A specific deluxe scaling will be introduced in subsection 3.6.

We can now define scaled operators $R_{D,\Gamma}^{(i)} := D^{(i)} R_\Gamma^{(i)}$ by pre-multiplying $R_\Gamma^{(i)}$ by the scaling matrices $D^{(i)}$. Other locally scaled operators $\widetilde{R}_{D,\Delta}^{(i)}$ are defined by

$\widetilde{R}^{(i)}_{D,\Delta} := R^{(i)}_{\Gamma\Delta} R^{(i)}_{D,\Gamma}$. We next consider a globally scaled operator $\widetilde{R}_{D,\Gamma}$ defined by the direct sum of $\widehat{R}_\Pi$ and all the $\widetilde{R}^{(i)}_{D,\Delta}$. We note that

$$\widetilde{R}^T_\Gamma \widetilde{R}_{D,\Gamma} = \widetilde{R}^T_{D,\Gamma} \widetilde{R}_\Gamma = I.$$

This identity shows that the averaging operator $E_D : \widetilde{W}_\Gamma \to \widetilde{W}_\Gamma$ given by

$$E_D := \widetilde{R}_\Gamma \widetilde{R}^T_{D,\Gamma} \tag{3.4}$$

is a projection. E_D provides a weighted average of the subdomain interface values across the interface Γ. We will provide details on our choice of scaling matrices in subsection 3.6.

3.3. **A block factorization.** The following block factorization of the inverse of the stiffness matrix is associated with the elimination of the interior degrees of freedom of all subdomains:

$$A^{-1} = \begin{bmatrix} I & -A_{II}^{-1} A_{I\Gamma} \\ 0 & I \end{bmatrix} \begin{bmatrix} A_{II}^{-1} & 0 \\ 0 & \widehat{S}_\Gamma^{-1} \end{bmatrix} \begin{bmatrix} I & 0 \\ -A_{I\Gamma}^T A_{II}^{-1} & I \end{bmatrix}. \tag{3.5}$$

Here $A_{I\Gamma} := (A_{I\Delta} \; A_{I\Pi})$. The Schur complement $\widehat{S}_\Gamma$, with respect to the interior unknowns, is positive definite and it can be obtained by sub-assembly

$$\widehat{S}_\Gamma := R_\Gamma^T S_\Gamma R_\Gamma = \sum_{i=1}^N R_\Gamma^{(i)T} S_\Gamma^{(i)} R_\Gamma^{(i)}, \tag{3.6}$$

where S_Γ is the direct sum of the local Schur complements defined by

$$S_\Gamma^{(i)} := A_{\Gamma\Gamma}^{(i)} - A_{I\Gamma}^{(i)T} A_{II}^{(i)-1} A_{I\Gamma}^{(i)},$$

and where

$$A_{\Gamma\Gamma}^{(i)} := \begin{bmatrix} A_{\Delta\Delta}^{(i)} & A_{\Delta\Pi}^{(i)} \\ A_{\Delta\Pi}^{(i)T} & A_{\Pi\Pi}^{(i)} \end{bmatrix}.$$

For the model problem (1.2), the local Schur complements $S_\Gamma^{(i)}$ are always positive definite. A preconditioner for (3.2) is then defined by using (3.5), after replacing the inverse of the Schur complement $\widehat{S}_\Gamma$ by the action of a suitable interface preconditioner.

3.4. **The BDDC algorithm.** In order to describe the BDDC algorithm, we need to define a partially assembled Schur complement, defined on $\widetilde{W}_\Gamma$, by

$$\widetilde{S}_\Gamma := \overline{R}_\Gamma^T S_\Gamma \overline{R}_\Gamma.$$

After eliminating the components of the right-hand side corresponding to the interior unknowns, we obtain

$$\widetilde{A} \begin{bmatrix} \boldsymbol{u}_I^{(1)} \\ \boldsymbol{u}_\Delta^{(1)} \\ \vdots \\ \boldsymbol{u}_I^{(N)} \\ \boldsymbol{u}_\Delta^{(N)} \\ \boldsymbol{u}_\Pi \end{bmatrix} = \begin{bmatrix} 0 \\ R_\Delta^{(1)} \widetilde{R}_{\Gamma\Delta} \widetilde{S}_\Gamma \boldsymbol{u}_\Gamma \\ \vdots \\ 0 \\ R_\Delta^{(N)} \widetilde{R}_{\Gamma\Delta} \widetilde{S}_\Gamma \boldsymbol{u}_\Gamma \\ \widetilde{R}_{\Gamma\Pi} \widetilde{S}_\Gamma \boldsymbol{u}_\Gamma \end{bmatrix},$$

where $\widetilde{A}$ is the partially assembled stiffness matrix on $W_I \oplus \widetilde{W}_\Gamma$. We note that solving this linear system is much less expensive than working with the fully assembled linear system since the number of primal variables is much smaller than the total number of interface variables. We also note that the fully assembled Schur complement $\widehat{S}_\Gamma$ can be obtained by an additional sub-assembly step, i.e., $\widehat{S}_\Gamma = \widetilde{R}_\Gamma^T \widetilde{S}_\Gamma \widetilde{R}_\Gamma$.

The BDDC preconditioner has the following form:

$$M^{-1} := \widetilde{R}_{D,\Gamma}^T \widetilde{S}_\Gamma^{-1} \widetilde{R}_{D,\Gamma}.$$

Here, $\widetilde{S}_\Gamma^{-1}$ can be obtained by using a block Cholesky factorization of $\widetilde{A}$ as in [50, section 4]:

(3.7)
$$\widetilde{S}_\Gamma^{-1} = \widetilde{R}_{\Gamma\Delta}^T \left(\sum_{i=1}^N \begin{bmatrix} 0 & R_\Delta^{(i)T} \end{bmatrix} \begin{bmatrix} A_{II}^{(i)} & A_{I\Delta}^{(i)} \\ A_{I\Delta}^{(i)T} & A_{\Delta\Delta}^{(i)} \end{bmatrix}^{-1} \begin{bmatrix} 0 \\ R_\Delta^{(i)} \end{bmatrix} \right) \widetilde{R}_{\Gamma\Delta} + \Phi S_{\Pi\Pi}^{-1} \Phi^T$$

with

$$\Phi := \widetilde{R}_{\Gamma\Pi}^T - \widetilde{R}_{\Gamma\Delta}^T \sum_{i=1}^N \begin{bmatrix} 0 & R_\Delta^{(i)T} \end{bmatrix} \begin{bmatrix} A_{II}^{(i)} & A_{I\Delta}^{(i)} \\ A_{I\Delta}^{(i)T} & A_{\Delta\Delta}^{(i)} \end{bmatrix}^{-1} \begin{bmatrix} A_{I\Pi}^{(i)} \\ A_{\Delta\Pi}^{(i)} \end{bmatrix} R_\Pi^{(i)}$$

and where

(3.8)
$$\begin{aligned} S_{\Pi\Pi} &:= \sum_{i=1}^N R_\Pi^{(i)T} S_{\Pi\Pi}^{(i)} R_\Pi^{(i)}, \\ S_{\Pi\Pi}^{(i)} &:= A_{\Pi\Pi}^{(i)} - \begin{bmatrix} A_{I\Pi}^{(i)T} & A_{\Delta\Pi}^{(i)T} \end{bmatrix} \begin{bmatrix} A_{II}^{(i)} & A_{I\Delta}^{(i)} \\ A_{I\Delta}^{(i)T} & A_{\Delta\Delta}^{(i)} \end{bmatrix}^{-1} \begin{bmatrix} A_{I\Pi}^{(i)} \\ A_{\Delta\Pi}^{(i)} \end{bmatrix}. \end{aligned}$$

The first term of (3.7) consists of uncoupled subdomain corrections realized by means of local Neumann solves, with solutions constrained to vanish at the primal degrees of freedom; the second term is the coarse-level part of the preconditioner associated with the primal space and provides the global exchange of information which is needed to obtain a scalable preconditioner for the conjugate gradient method. In subsection 3.8, we will also explore the option of approximating the inverse of $S_{\Pi\Pi}$ by invoking the BDDC algorithm once more, thus introducing a three-level BDDC algorithm.

3.5. **Interface equivalence classes.** Equivalence classes of degrees of freedom related to the interface between the subdomains play an important role in the design, analysis, and parallel implementation of domain decomposition algorithms such as BDDC. In the case of $H(\mathrm{div})-$conforming Raviart-Thomas and BDM elements, the situation is very simple since each interface degree of freedom is associated with an element face common to only two elements. Thus, any equivalence class will be given by the subset of the degrees of freedom on the intersection of the boundaries of two neighboring subdomains. We will refer to such an interface class as a subdomain face. In order to avoid disconnected subdomain faces in our experiments, we will consider two degrees of freedom connected and belonging to the same subdomain face only if there exists a path between their element faces which passes from element to element of the subdomain face crossing edges between element faces.

3.6. **Deluxe scaling.** In order to complete the description of the algorithm, we need to define the weighted averaging operators $D^{(i)}$. Conventional weighted averaging techniques, known as stiffness and ρ scalings, are described in [21, 56]. We will show, in section 5, that there are cases for which these conventional techniques perform poorly for (1.2), since these methods are designed for constant coefficients or for one variable coefficient. For more than one variable coefficient, as for the problem considered here, we need a different approach and we will use the deluxe scaling, introduced in [25] for $H(\mathbf{curl})$ problems and further considered in [26]. A survey of other studies using deluxe scaling is given in [83].

We will work with the principal minors, associated with the subdomain faces F, of the subdomain stiffness matrices. Two local stiffness matrices associated with F are given by principal minors of the subdomain stiffness matrices

$$\begin{bmatrix} A_{II}^{(k)} & A_{IF}^{(k)} \\ A_{IF}^{(k)T} & A_{FF}^{(k)} \end{bmatrix}, \ k = i, j,$$

and the two Schur complements associated with F by

$$S_{FF}^{(k)} := A_{FF}^{(k)} - A_{IF}^{(k)T} {A_{II}^{(k)}}^{-1} A_{IF}^{(k)}, \ k = i, j.$$

We will use the scaling matrices $D_F^{(i)} := \left(S_{FF}^{(i)} + S_{FF}^{(j)}\right)^{-1} S_{FF}^{(i)}$. The deluxe scaling operator $D^{(i)}$ is then given by

$$D^{(i)} := \begin{bmatrix} D_{F_1}^{(i)} & & & \\ & D_{F_2}^{(i)} & & \\ & & \ddots & \\ & & & D_{F_k}^{(i)} \end{bmatrix}, \tag{3.9}$$

where $F_1, \ldots, F_k$ are the subdomain faces of Γ_i.

We remark that there are two scaling matrices for each subdomain face, and that it is easy to show that the partition of unity condition (3.3) is satisfied, i.e., that

$$\sum_{i=1}^{N} {R_\Gamma^{(i)}}^T D^{(i)} R_\Gamma^{(i)} = I.$$

Thus, a face component of the averaging operator E_D is defined by

$$\bar{\boldsymbol{w}}_F := (E_D \boldsymbol{w})_F := (S_{FF}^{(i)} + S_{FF}^{(j)})^{-1} (S_{FF}^{(i)} \boldsymbol{w}_F^{(i)} + S_{FF}^{(j)} \boldsymbol{w}_F^{(j)}).$$

Here $\boldsymbol{w}_F^{(i)}$ (resp. $\boldsymbol{w}_F^{(j)}$) is the restriction of $\boldsymbol{w}^{(i)} \in W_\Gamma^{(i)}$ ($\boldsymbol{w}^{(j)} \in W_\Gamma^{(j)}$) to the face F.

The action of $(S_{FF}^{(i)} + S_{FF}^{(j)})^{-1}$ can be implemented by solving a Dirichlet problem on $\Omega_i \cup F \cup \Omega_j$, where F is the face between the two subdomains. This can add significantly to the cost. In the economic variant of deluxe scaling (e-deluxe), we replace this large domain by a thin domain built from one or a few layers of elements next to the face and this often results in very similar performance; see, e.g., [26] and section 5. Instead of solving such a Dirichlet problem, in our experiments, we exploit the Schur complement feature of the numerical factorization package MUMPS [2], which explicitly provides the local Schur complement matrix $S_\Gamma^{(i)}$ when factoring the subdomain problem. Our approach has the further advantage that the Dirichlet solver can be reused in the static condensation step in (3.5), and that the Schur

complement solver can be reused when computing the subdomain correction in (3.7). Therefore, a single factorization step suffices to set up the preconditioner.

Differently from [26], in our experiments with the e-deluxe variant, we consider the principal minors of the Schur complement obtained by eliminating all the interior degrees of freedom in a layer of elements next to all of the subdomain interface Γ_i. However, when using e-deluxe, the Dirichlet and Schur complement solvers cannot be reused, and additional factorizations are needed to set up the preconditioner. We note that our implementation of e-deluxe is quite similar to the one analyzed in [40].

3.7. **Basic BDDC deluxe estimates.** As we have previously noted, the Raviart–Thomas discretization only has equivalence classes with two elements. Therefore, the analysis will be quite similar to that for finite element problems for standard elliptic problems in two dimensions; see e.g., [40] or [68].

The core of any estimate for a BDDC algorithm is an estimate of the norm of the averaging operator E_D. By an algebraic argument, known for FETI–DP since 2002, we have

$$\kappa(M^{-1}\widehat{S}_\Gamma) \leq \|E_D\|_{\widetilde{S}_\Gamma};$$

see [43] or [50]. The analysis of any BDDC deluxe algorithm can be reduced to bounds for individual subdomains. Arbitrary jumps in the coefficients across Γ can then be accommodated.

Instead of developing an estimate for E_D, we will work with $P_D := I - E_D$. As shown in [68, Appendix A] these two operators, in fact, have the same norm. Thus, we will estimate the $S_\Gamma^{(i)}$–norm of $R_F^T(\boldsymbol{w}_F^{(i)} - \bar{\boldsymbol{w}}_F)$, instead of $(R_F^T\bar{\boldsymbol{w}}_F)^T S_\Gamma^{(i)} R_F^T\bar{\boldsymbol{w}}_F$. Here R_F denotes the restriction to the face F. By elementary algebra, we find that

$$\boldsymbol{w}_F^{(i)} - \bar{\boldsymbol{w}}_F = (S_{FF}^{(i)} + S_{FF}^{(j)})^{-1} S_{FF}^{(j)}(\boldsymbol{w}_F^{(i)} - \boldsymbol{w}_F^{(j)}).$$

More algebra gives, by using that $S_{FF}^{(i)} := R_F S_\Gamma^{(i)} R_F^T$,

$$(R_F^T(\boldsymbol{w}_F^{(i)} - \bar{\boldsymbol{w}}_F))^T S_\Gamma^{(i)}(R_F^T(\boldsymbol{w}_F^{(i)} - \bar{\boldsymbol{w}}_F))$$
$$= (\boldsymbol{w}_F^{(i)} - \boldsymbol{w}_F^{(j)})^T S_{FF}^{(j)}(S_{FF}^{(i)} + S_{FF}^{(j)})^{-1} S_{FF}^{(i)}(S_{FF}^{(i)} + S_{FF}^{(j)})^{-1} S_{FF}^{(j)}(\boldsymbol{w}_F^{(i)} - \boldsymbol{w}_F^{(j)}).$$

Adding a similar contribution from Ω_j, we obtain, following Pechstein and Dohrmann [67], that the relevant expression of the energy is

$$(\boldsymbol{w}_F^{(i)} - \boldsymbol{w}_F^{(j)})^T (S_{FF}^{(i)^{-1}} + S_{FF}^{(j)^{-1}})^{-1}(\boldsymbol{w}_F^{(i)} - \boldsymbol{w}_F^{(j)}).$$

The matrix of this quadratic form is a *parallel sum*, and we will use the notation

$$A : B := (A^{-1} + B^{-1})^{-1};$$

cf. [5].

We now use the following result; see [4, Theorem 9], see also [68, Corollary 5.11]:

Lemma 3.1. *Let A and B be two symmetric positive semi-definite matrices of the same order. Then, $z^T A : B z = \inf_{z=x+y}(x^T A x + y^T B y)$.*

By using $x = \boldsymbol{w}_F^{(i)} - \boldsymbol{w}_\Pi$ and $y = -\boldsymbol{w}_F^{(j)} + \boldsymbol{w}_\Pi$, where $\boldsymbol{w}_\Pi$ is an arbitrary element of the primal space, we find that

$$(\boldsymbol{w}_F^{(i)} - \boldsymbol{w}_F^{(j)})^T (S_{FF}^{(i)} : S_{FF}^{(j)})(\boldsymbol{w}_F^{(i)} - \boldsymbol{w}_F^{(j)})$$
$$\leq (\boldsymbol{w}_F^{(i)} - \boldsymbol{w}_\Pi)^T S_{FF}^{(i)}(\boldsymbol{w}_F^{(i)} - \boldsymbol{w}_\Pi) + (\boldsymbol{w}_F^{(j)} - \boldsymbol{w}_\Pi)^T S_{FF}^{(j)}(\boldsymbol{w}_F^{(j)} - \boldsymbol{w}_\Pi).$$

We note that each of these terms is local to only one subdomain.

In Lemma 4.8, we will establish a bound for $(\boldsymbol{w}_F^{(i)} - \boldsymbol{w}_\Pi)^T S_{FF}^{(i)} (\boldsymbol{w}_F^{(i)} - \boldsymbol{w}_\Pi)$ by the energy $a_i(\boldsymbol{w}^{(i)}, \boldsymbol{w}^{(i)})$ attributable to Ω_i, for a primal space element $\boldsymbol{w}_\Pi$ chosen to satisfy the no-net-flux condition

$$\int_F (\boldsymbol{w}_F^{(i)} - \boldsymbol{w}_\Pi) \cdot \boldsymbol{n} \, ds = 0,$$

for each subdomain face.

When developing this bound, we have to make sure that they hold for any extension of the values of $\boldsymbol{w}_F^{(i)}$ to the rest of Γ_i. This will be done by considering the energy-minimizing extension of any finite element function defined on F.

The relevant matrix is $\breve{S}_{FF}^{(i)}$, defined by

$$\breve{S}_{FF}^{(i)} := S_{FF}^{(i)} - S_{F'F}^{(i)T} S_{F'F'}^{(i)-1} S_{F'F}^{(i)}, \tag{3.10}$$

where $S_{F'F'}^{(i)}$ is the principal minor of $S_\Gamma^{(i)}$ with respect to $\Gamma_i \setminus F$ and $S_{F'F}^{(i)}$ an off-diagonal block of $S_\Gamma^{(i)}$. Thus, $\boldsymbol{w}_F^{(i)T} \breve{S}_{FF}^{(i)} \boldsymbol{w}_F^{(i)}$ provides a lower bound for $a_i(\boldsymbol{w}, \boldsymbol{w})$.

In standard BDDC theory, as in section 4, the required estimate is obtained by using a *face lemma*, cf. [75, subsection 4.6.3], where such a result is established for constant coefficients in each subdomain, polyhedral subdomains, and scalar elliptic problems. For an adaptive algorithm, this result is replaced by the use of a generalized eigenvalue problem. For BDDC deluxe, we first generate elements for the primal space for a face by solving a generalized eigenvalue problem

$$S_{FF}^{(i)} : S_{FF}^{(j)} \psi = \nu \breve{S}_{FF}^{(i)} : \breve{S}_{FF}^{(j)} \psi. \tag{3.11}$$

The primal spaces are then generated by the eigenvectors for one or a few of the largest eigenvalues of (3.11) and making $(\breve{S}_{FF}^{(i)} : \breve{S}_{FF}^{(j)})(\boldsymbol{w}_F^{(i)} - \boldsymbol{w}_F^{(j)})$ orthogonal to these eigenvectors. The complementary dual space is then spanned by the remaining eigenvectors which are then orthogonal to the primal space with respect to the matrix $\breve{S}_{FF}^{(i)} : \breve{S}_{FF}^{(j)}$.

We note that since $\boldsymbol{w}_F^{(i)} - \boldsymbol{w}_F^{(j)}$ belongs to the dual space

$$(\boldsymbol{w}_F^{(i)} - \boldsymbol{w}_F^{(j)})^T (S_{FF}^{(i)} : S_{FF}^{(j)})(\boldsymbol{w}_F^{(i)} - \boldsymbol{w}_F^{(j)}) \leq \nu_{tol}^F (\boldsymbol{w}_F^{(i)} - \boldsymbol{w}_F^{(j)})^T (\breve{S}_{FF}^{(i)} : \breve{S}_{FF}^{(j)})(\boldsymbol{w}_F^{(i)} - \boldsymbol{w}_F^{(j)}),$$

where ν_{tol}^F is the largest eigenvalue not used in the selection of primal constraints. Using Lemma 3.1, once more, choosing $x = \boldsymbol{w}_F^{(i)}$ and $y = -\boldsymbol{w}^{(j)}$, we have established the following result.

Lemma 3.2. *If ν_{tol}^F is the largest eigenvalue not used in the selection of primal constraints, we have*

$$\|(P_D \boldsymbol{w})_{|F}\|_{\widetilde{S}_\Gamma}^2 \leq \nu_{tol}^F (a_i(\boldsymbol{w}, \boldsymbol{w}) + a_j(\boldsymbol{w}, \boldsymbol{w})),$$

where $a_i(\cdot, \cdot)$ is given by (3.1).

We now note that we can write $P_D \boldsymbol{w}$ as the sum of contributions $(P_D \boldsymbol{w})_{|F}$ from the faces of Γ. An estimate of the square of the norm of the sum related to one subdomain Ω_i introduces a factor N_F, the maximum number of faces of any subdomain. Counting the number of contributions of the form $a_i(\boldsymbol{w}, \boldsymbol{w})$, we then obtain the following result:

Theorem 3.3. *$\kappa(M^{-1} \widehat{S}_\Gamma) \leq \|P_D\|_{\widetilde{S}_\Gamma} \leq \nu_{tol} N_F^2$, where $\nu_{tol} := \max_F \nu_{tol}^F$ and N_F equals the maximum number of faces of any subdomain.*

We note that this bound is often pessimistic, because of the factor N_F^2; when using a tolerance in our computations, we therefore have chosen to disregard this factor.

We also note that there is evidence that adaptive primal spaces for deluxe BDDC methods are smaller than those generated using conventional point-wise scalings [38, 40, 90]. See also the discussion in [68, Lemma 5.24].

3.8. **Three-level BDDC.** Coarse problem solvers in BDDC methods, as in all other two-level Domain Decomposition methods, can create a bottleneck for the algorithm when there is a large number of subdomains and/or many coarse degrees of freedom per subdomain, as could be the case when an adaptive BDDC algorithm is used. A multilevel extension of the BDDC algorithm is readily available given the unassembled nature of the coarse problem (3.8); for a pioneering analysis see [78, 79].

In a three-level BDDC algorithm, the solution of the coarse problem is replaced by the application of a BDDC preconditioner at a coarser level, where a fine subdomain is considered an element of a coarser mesh, with $S_{\Pi\Pi}^{(i)}$ the coarse element stiffness matrices. Coarse subdomains are then obtained by partitioning the connectivity graph of the coarse mesh, where two coarse elements are considered connected if they share at least one fine subdomain face. We note that we can iterate this procedure to construct BDDC algorithms with an arbitrary number of levels.

Such multilevel extensions lead to highly scalable, memory efficient BDDC preconditioners, provided a suitable coarse space for the coarser level is found. In fact, the use of approximate coarse solvers contributes multiplicatively to the condition number of the BDDC algorithm, and can increase the number of iterations of the Krylov solver, since the following upper bound for the condition number of a three-level BDDC method holds, cf. [22, Theorem 1],

$$\kappa(M_{3level}^{-1}\widehat{S}_\Gamma) \leq \kappa(M_{\Pi\Pi}^{-1}S_{\Pi\Pi})\kappa(M^{-1}\widehat{S}_\Gamma),$$

where $M_{\Pi\Pi}^{-1}$ is the BDDC preconditioner for $S_{\Pi\Pi}$. We note that this result of Dohrmann contains a factor

$$\frac{\alpha_2 \max(1,\beta_2)}{\alpha_1 \min(1,\beta_1)}.$$

A closer examination shows that in our case $\alpha_1 = \alpha_2 = 1$, that $\beta_1 = 1$, that $\beta_2 \geq 1$, and that $\kappa(M_{\Pi\Pi}^{-1}S_{\Pi\Pi}) = \beta_2/\beta_1$.

Differently from earlier work, we will construct an adaptive coarse problem for $S_{\Pi\Pi}$ and will then be able to control $\kappa(M_{\Pi\Pi}^{-1}S_{\Pi\Pi})$ and construct highly scalable, memory efficient three-level BDDC preconditioners. We note that the design of effective primal spaces for coarser levels of $H(\mathrm{div})$ problems could be a subject of future development of theory.

4. Technical tools and the main theoretical result

When we turn to the development of our theory, we need to impose additional conditions on the geometry of the subdomains and the values of the two material parameters α and β. Thus, each subdomain Ω_i will be assumed to be convex and a union of a finite number of shape-regular tetrahedral elements of a coarse triangulation $\mathcal{T}_H$. The mesh of each subdomain will be quasi-uniform. We also assume that α and β are constant in each subdomain while we allow arbitrarily large coefficient jumps across the interface. We will denote by α_i and β_i the values of these

coefficients taken on subdomain Ω_i. We note that similar assumptions have been used in the development of theory for many domain decomposition algorithms of the iterative substructuring family; see, e.g., [75, Chapters 4–6].

Our primal variables will be defined by the common average of the normal component of the solution over the subdomain faces. This means that a no-net-flux condition

$$\int_F \boldsymbol{w}_\Delta^{(i)} \cdot \boldsymbol{n} \, ds = 0$$

is imposed for each subdomain face.

In our proofs, we also need some standard tools for the space $S(\Omega_i)$, which we can borrow from [75, subsection 4.6]. These results are related to the subdomain faces and their boundaries. We note that the proof of [75, Lemma 4.16] is not satisfactory but that a correct proof is now available in [26, Section 3.].

Lemma 4.1. *There are functions $\vartheta_{\partial F} \in S(\Omega_i)$ and $\vartheta_F \in S(\Omega_i)$ such that for all nodes on the closure of F*

$$0 \leq \vartheta_{\partial F}, \quad \vartheta_F \leq 1, \quad \vartheta_{\partial F} + \vartheta_F = 1,$$

$\vartheta_F = 0$ on $\partial\Omega_i \backslash F$, and $\vartheta_{\partial F} = 0$ at all nodes of $\partial\Omega_i$ except those on ∂F. Moreover, for any $u \in S(\Omega_i)$, there exists a constant independent of h_i and H_i, such that

$$|I_h(\vartheta_{\partial F} u)|^2_{1;\Omega_i} \leq C\,(1 + \log H_i/h_i)\,\|u\|^2_{1;\Omega_i}$$

and

$$|I_h(\vartheta_F u)|^2_{1;\Omega_i} \leq C\,(1 + \log H_i/h_i)^2\,\|u\|^2_{1;\Omega_i}\,.$$

In addition, the following estimates hold:

$$\|u\|^2_{0;\partial F} \leq C\,(1 + \log H_i/h_i)\,\|u\|^2_{1;\Omega_i}$$

and

$$\|I_h(\vartheta_F u)\|_{0,\Omega_i} \leq \|u\|_{0,\Omega_i}.$$

We note that an explicit construction of ϑ_F, a nonnegative function bounded from above by 1, is given in [75, Subsection 4.6.3] for a tetrahedron. This construction can easily be extended to the union of several coarse elements.

We next introduce a stable operator, which provides a divergence-free extension.

Lemma 4.2 (Divergence-free extension)**.** *There exists an extension operator $\widetilde{\mathcal{H}}_i$ from the normal trace space of $W_\Delta^{(i)}$ to $W^{(i)}$, such that, for all $\boldsymbol{u} \in W_\Delta^{(i)}$,*

$$\left(\widetilde{\mathcal{H}}_i \mu\right) \cdot \boldsymbol{n} = \mu, \ \operatorname{div} \widetilde{\mathcal{H}}_i \mu = 0,$$

where $\mu := \boldsymbol{u} \cdot \boldsymbol{n}$. Moreover,

$$\left\|\widetilde{\mathcal{H}}_i \mu\right\|_{0;\Omega_i} \leq C\,\|\mu\|_{-1/2;\partial\Omega_i}\,.$$

Proof. A proof of this result is provided for the lowest order Raviart-Thomas element defined on hexahedral meshes in [85, Lemma 4.3] and [84, Lemma 2.6]. A proof for the case of tetrahedral elements can be obtained using exactly the same arguments. □

We then have the following estimate for the discrete harmonic extension, i.e., the extension of a given normal trace with the minimal energy. For more details, see [75, section 10.2] and [63, section 3.1].

Corollary 4.3 (Discrete harmonic extension)**.** *Let $\mathcal{H}_i$ be the energy minimizing discrete harmonic extension. For all $\boldsymbol{u} \in W_{\Delta}^{(i)}$, we have*

$$(\mathcal{H}_i \mu) \cdot \boldsymbol{n} = \mu := \boldsymbol{u} \cdot \boldsymbol{n}.$$

Furthermore,

$$\alpha_i \left\| \operatorname{div} \mathcal{H}_i \mu \right\|_{0;\Omega_i}^2 + \beta_i \left\| \mathcal{H}_i \mu \right\|_{0;\Omega_i}^2 \leq C \beta_i \left\| \mu \right\|_{-1/2;\partial\Omega_i}^2 .$$

Proof. $\mathcal{H}_i$ is the minimal-energy extension operator for a given subdomain interface. Therefore, we have

$$\alpha_i \left\| \operatorname{div} \mathcal{H}_i \mu \right\|_{0;\Omega_i}^2 + \beta_i \left\| \mathcal{H}_i \mu \right\|_{0;\Omega_i}^2 \leq \alpha_i \left\| \operatorname{div} \widetilde{\mathcal{H}}_i \mu \right\|_{0;\Omega_i}^2 + \beta_i \left\| \widetilde{\mathcal{H}}_i \mu \right\|_{0;\Omega_i}^2 .$$

Since $\operatorname{div} \widetilde{\mathcal{H}}_i \mu = 0$, we have, by using Lemma 4.2,

$$\alpha_i \left\| \operatorname{div} \mathcal{H}_i \mu \right\|_{0;\Omega_i}^2 + \beta_i \left\| \mathcal{H}_i \mu \right\|_{0;\Omega_i}^2 \leq C \beta_i \left\| \mu \right\|_{-1/2;\partial\Omega_i}^2 .$$

□

We next consider a coarse interpolation operator ρ_H^{RT} onto the Raviart-Thomas space on the coarse mesh $\mathcal{T}_H$.

Lemma 4.4 (Stability of the coarse interpolant)**.** *Let $K \in \mathcal{T}_H$. For all $\boldsymbol{u} \in W$, we have the following estimates:*

$$\left\| \operatorname{div} \left(\rho_H^{RT} \boldsymbol{u} \right) \right\|_{0;K}^2 \leq \left\| \operatorname{div} \boldsymbol{u} \right\|_{0;K}^2$$

and

$$\left\| \rho_H^{RT} \boldsymbol{u} \right\|_{0;K}^2 \leq C \left((1 + \log H/h) \left\| \boldsymbol{u} \right\|_{0;K}^2 + H_K^2 \left\| \operatorname{div} \boldsymbol{u} \right\|_{0;K}^2 \right),$$

where H_K is the diameter of K. Here, the constant C depends only on the aspect ratio of K and the elements of $\mathcal{T}_h$.

Proof. Full proofs of this result are given in [84, Lemma 2.4] and [85, Lemma 4.1] for hexahedral meshes. These proofs can be translated line by line to also hold for tetrahedral meshes. □

We then have the following.

Lemma 4.5. *Let $\boldsymbol{u}_F \in W^{(i)}$ with $\lambda_f (\boldsymbol{u}_F) = 0, \forall f \subset \partial\Omega_i \backslash F$. Furthermore, let $\boldsymbol{u}_F^H := \mathcal{H}_i \left(\rho_H^{RT} \boldsymbol{u}_F \cdot \boldsymbol{n} \right)$ and assume that $\alpha_i \leq \beta_i H_i^2$. We then have for the bilinear form* (3.1)

$$a_i \left(\boldsymbol{u}_F^H, \boldsymbol{u}_F^H \right) \leq C a_i \left(\boldsymbol{u}_F, \boldsymbol{u}_F \right), \tag{4.1}$$

where C is independent of H_i, h_i, α_i, and β_i.

Proof. We will modify the proof of [63, Lemma 5.6]. We first assume that F consists of only one face of a coarse element $K \in \mathcal{T}_H \subset \Omega_i$. Let $\Omega_{i,F}^{d_i} \subset \Omega_i$ be the set of all points which are within a distance d_i of F. Let χ_F be a piecewise linear, scalar, nonnegative cut-off function, which has the value 1 on F and vanishes in $\Omega_i \backslash \Omega_{i,F}^{d_i}$ for some $h_i \leq d_i \leq H_i$. Moreover, $\left\| \chi_F \right\|_{\infty} \leq 1$ and $\left\| \nabla \chi_F \right\|_{\infty} \leq C/d_i$.

We next consider a coarse basis function related to a discrete harmonic extension. This basis function $\widetilde{\boldsymbol{\phi}}_F^{RT}$ is obtained from the standard basis function $\boldsymbol{\phi}_F^{RT}$ and is given by $\widetilde{\boldsymbol{\phi}}_F^{RT} := \mathcal{H}_i \left(\chi_F \boldsymbol{\phi}_F^{RT} \cdot \boldsymbol{n} \right)$. We note that $\left\| \boldsymbol{\phi}_F^{RT} \right\|_{0;\Omega_i}^2 \leq C H_i^3$ and $\left\| \operatorname{div} \boldsymbol{\phi}_F^{RT} \right\|_{0;\Omega_i}^2 \leq C H_i$.

We then define the function $\widetilde{\boldsymbol{u}}_F^H$ as follows:

$$\widetilde{\boldsymbol{u}}_F^H := \lambda_F(\boldsymbol{u}_F)\,\widetilde{\boldsymbol{\phi}}_F^{RT}. \tag{4.2}$$

In order to estimate the energy of $\widetilde{\boldsymbol{u}}_F^H$, we will estimate the coefficient $\lambda_F(\boldsymbol{u}_F)$ and the energy of $\widetilde{\boldsymbol{\phi}}_F^{RT}$, separately.

We first estimate the coefficient. By the divergence theorem, and the fact that $(\chi_F \boldsymbol{u}_F)\cdot\boldsymbol{n}$ vanishes on $\partial\Omega_{i,F}^{d_i}\backslash F$,

$$\begin{aligned}
|F|\,\lambda_F(\boldsymbol{u}_F) = |F|\,\lambda_F(\chi_F\boldsymbol{u}_F) &= \int_F (\chi_F\boldsymbol{u}_F)\cdot\boldsymbol{n}\,ds \\
&= \int_{\Omega_{i,F}^{d_i}} \operatorname{div}(\chi_F\boldsymbol{u}_F)\,dx - \int_{\partial\Omega_{i,F}^{d_i}\backslash F} (\chi_F\boldsymbol{u}_F)\cdot\boldsymbol{n}\,ds \\
&= \int_{\Omega_{i,F}^{d_i}} \operatorname{div}(\chi_F\boldsymbol{u}_F)\,dx.
\end{aligned}$$

By using the Cauchy-Schwarz inequality and the shape-regularity of the elements of $\mathcal{T}_H$, we obtain

$$\begin{aligned}
|\lambda_F(\boldsymbol{u}_F)|^2 &\le C\frac{d_i}{H_i^2}\,\|\operatorname{div}(\chi_F\boldsymbol{u}_F)\|^2_{0;\Omega_{i,F}^{d_i}} \\
&\le C\frac{d_i}{H_i^2}\left(\|\chi_F\|^2_\infty\,\|\operatorname{div}\boldsymbol{u}_F\|^2_{0;\Omega_i} + \|\nabla\chi_F\|^2_\infty\,\|\boldsymbol{u}_F\|^2_{0;\Omega_i}\right) \\
&\le C\frac{d_i}{H_i^2}\,\|\operatorname{div}\boldsymbol{u}_F\|^2_{0;\Omega_i} + C\frac{1}{H_i^2 d_i}\,\|\boldsymbol{u}_F\|^2_{0;\Omega_i}.
\end{aligned}$$

We are now ready to obtain our estimate of the basis function. From the minimal energy property, we find

$$\begin{aligned}
&\alpha_i\left\|\operatorname{div}\widetilde{\boldsymbol{\phi}}_F^{RT}\right\|^2_{0;\Omega_i} + \beta_i\left\|\widetilde{\boldsymbol{\phi}}_F^{RT}\right\|^2_{0;\Omega_i} \\
&\le \alpha_i\left\|\operatorname{div}\left(\rho_h^{RT}\left(\chi_F\boldsymbol{\phi}_F^{RT}\right)\right)\right\|^2_{0;\Omega_i} + \beta_i\left\|\left(\rho_h^{RT}\left(\chi_F\boldsymbol{\phi}_F^{RT}\right)\right)\right\|^2_{0;\Omega_i} \\
&\le C\alpha_i\left(d_i + H_i^2/d_i\right) + C\beta_i H_i^2 d_i \le C\alpha_i H_i^2/d_i + C\beta_i H_i^2 d_i.
\end{aligned}$$

Hence, we have

$$\begin{aligned}
a_i\left(\widetilde{\boldsymbol{u}}_F^H,\widetilde{\boldsymbol{u}}_F^H\right) &= \alpha_i\left\|\lambda_F(\boldsymbol{u}_F)\left(\operatorname{div}\widetilde{\boldsymbol{\phi}}_F^{RT}\right)\right\|^2_{0;\Omega_i} + \beta_i\left\|\lambda_F(\boldsymbol{u}_F)\left(\widetilde{\boldsymbol{\phi}}_F^{RT}\right)\right\|^2_{0;\Omega_i} \\
&\le C\left(\alpha_i + \beta_i d_i^2\right)\|\operatorname{div}\boldsymbol{u}_F\|^2_{0;\Omega_i} + C\left(\alpha_i/d_i^2 + \beta_i\right)\|\boldsymbol{u}_F\|^2_{0;\Omega_i}.
\end{aligned} \tag{4.3}$$

Let $d_i = \max\{\sqrt{\alpha_i/\beta_i}, h_i\}$ and recall that $h_i \le d_i \le H_i$. By using (4.3) and Lemma 2.3, we obtain

$$a_i\left(\boldsymbol{u}_F^H,\boldsymbol{u}_F^H\right) \le a_i\left(\widetilde{\boldsymbol{u}}_F^H,\widetilde{\boldsymbol{u}}_F^H\right) \le C a_i(\boldsymbol{u}_F,\boldsymbol{u}_F).$$

If F is the union of faces of several elements of $\mathcal{T}_H$, we should replace the basis function in formula (4.2) by a sum of such functions associated with the relevant faces of the coarse elements. □

We next introduce a partition of unity associated with the faces of an individual subdomain Ω_i as in [75, Chapter 10.2.1],

$$\sum_{F\subset\partial\Omega_i} \zeta_F = 1, \text{a.e. on } \partial\Omega_i\backslash\partial\Omega,$$

where

$$\zeta_F(x) := \begin{cases} 1, & x \in F, \\ 0, & x \in \partial\Omega_i \backslash F. \end{cases} \tag{4.4}$$

We then have the following estimates for the subdomain face components; we recall that for $\boldsymbol{u}_i \in W_\Delta^{(i)}$, $\int_F \boldsymbol{u}_i \cdot \boldsymbol{n}\, ds = 0$ for each subdomain face $F \subset \partial\Omega_i$.

Lemma 4.6. *For any $\boldsymbol{u}_i \in W_\Delta^{(i)}$ and for any $\boldsymbol{u}_i^H \in W_\Pi^{(i)}$, let $\mu_i := \boldsymbol{u}_i \cdot \boldsymbol{n}$, $\mu_F := \zeta_F \mu_i$, and $\mu_i^H := \boldsymbol{u}_i^H \cdot \boldsymbol{n}$. Then, the following estimate holds:*

$$\begin{aligned} &\|\mu_F\|^2_{-1/2;\partial\Omega_i} \\ &\quad \leq C\,(1+\log H_i/h_i)\left((1+\log H_i/h_i)\left\|\mu_i+\mu_i^H\right\|^2_{-1/2;\partial\Omega_i} + \|\mu_i\|^2_{-1/2;\partial\Omega_i}\right), \end{aligned}$$

where C is independent of μ_i^H, H_i, and h_i.

Proof. This result is closely related to [85, Lemma 4.4] and [84, Lemma 2.7], which are results for hexahedral meshes. Carefully checking all the arguments, we find that the same results are also valid for tetrahedral meshes. □

Unlike for the gradient operator, it is quite complicated to classify the kernel and the range of the curl and divergence operators. The discrete regular decompositions given in [35] provide useful tools to analyze problems posed in $H(\mathbf{curl})$ and $H(\mathrm{div})$. We can then apply techniques developed for H^1-functions by using the following result.

Lemma 4.7 (Hiptmair-Xu decomposition)**.** *Let $\mathcal{D} \subset \Omega$ be a convex polyhedron. Then, for all $\boldsymbol{v}_h \in W(\mathcal{D})$, there exist $\boldsymbol{\Psi}_h \in S(\mathcal{D})$, $\boldsymbol{q}_h \in X(\mathcal{D})$, and $\widetilde{\boldsymbol{v}}_h \in W(\mathcal{D})$ such that*

$$\boldsymbol{v}_h = \widetilde{\boldsymbol{v}}_h + \rho_h^{RT}(\boldsymbol{\Psi}_h) + \mathbf{curl}\,\boldsymbol{q}_h,$$

and

$$\left\|h_i^{-1}\widetilde{\boldsymbol{v}}_h\right\|^2_{0;\mathcal{D}} + \|\boldsymbol{\Psi}_h\|^2_{1;\mathcal{D}} \leq C\,\|\mathrm{div}\,\boldsymbol{v}_h\|^2_{0;\mathcal{D}}, \tag{4.5}$$

$$\|\mathbf{curl}\,\boldsymbol{q}_h\|^2_{0;\mathcal{D}} + \|\boldsymbol{\Psi}_h\|^2_{0;\mathcal{D}} \leq C\,\|\boldsymbol{v}_h\|^2_{0;\mathcal{D}}. \tag{4.6}$$

Proof. See [35, Lemmas 5.1 and 5.2]. □

We note that this important paper, [35], was preceded by [34], which concerns another application of the same decomposition.

We are now ready to prove a face lemma for Raviart–Thomas finite elements, which according to our results in subsection 3.7 will allow us to complete the proof of our main theoretical result.

Lemma 4.8. *For any $\boldsymbol{u}_i \in W^{(i)}$, there exist $\boldsymbol{v}_{i,F} \in W^{(i)}$ and $\boldsymbol{v}_{i,F}^H \in W_\Pi^{(i)}$ such that*

$$\begin{cases} \lambda_f(\boldsymbol{v}_{i,F}) = \lambda_f(\boldsymbol{u}_i) & \text{if } f \subset F, \\ \lambda_f(\boldsymbol{v}_{i,F}) = 0 & \text{if } f \subset \partial\Omega_i \backslash F, \end{cases} \tag{4.7}$$

and

$$\begin{cases} \lambda_f\left(\boldsymbol{v}_{i,F}^H\right) = \lambda_f\left(\rho_H^{RT}\boldsymbol{u}_i\right) & \text{if } f \subset F, \\ \lambda_f\left(\boldsymbol{v}_{i,F}^H\right) = 0 & \text{if } f \subset \partial\Omega_i \backslash F. \end{cases} \tag{4.8}$$

Furthermore,

$$a_i\left(\boldsymbol{v}_{i,F}-\boldsymbol{v}_{i,F}^H,\boldsymbol{v}_{i,F}-\boldsymbol{v}_{i,F}^H\right)\leq C\left(1+\log H_i/h_i\right)^2 a_i\left(\boldsymbol{u}_i,\boldsymbol{u}_i\right), \tag{4.9}$$

where C is independent of α_i, β_i, H_i, and h_i.

Proof. We will only consider the case where $\alpha_i \leq \beta_i H_i^2$ since for $\beta_i H_i^2 \leq \alpha_i$, the proof is straightforward by using Corollary 4.3 and Lemmas 4.6, 2.1, and 4.4; for more details, see [85, Section 5].

By using Lemma 4.7, we can find $\widetilde{\boldsymbol{u}}_i$, $\boldsymbol{\Psi}_i$, and $\boldsymbol{q}_i$ such that

$$\boldsymbol{u}_i=\widetilde{\boldsymbol{u}}_i+\rho_h^{RT}\left(\boldsymbol{\Psi}_i\right)+\mathbf{curl}\,\boldsymbol{q}_i=\boldsymbol{u}_i^1+\boldsymbol{u}_i^2+\boldsymbol{u}_i^3. \tag{4.10}$$

We note that $\operatorname{div}\left(\mathbf{curl}\,\boldsymbol{q}_i\right)=0$ and that (4.5) and (4.6) provide bounds for the different terms. Based on the decomposition, we will explicitly construct $\boldsymbol{v}_{i,F}$ and $\boldsymbol{v}_{i,F}^H$ in the following form:

$$\begin{aligned}\boldsymbol{v}_{i,F}&=\widetilde{\boldsymbol{u}}_{i,F}+\left(\rho_h^{RT}\left(\boldsymbol{\Psi}_{i,F}\right)+\boldsymbol{\Psi}_{i,\partial F}\right)+\left(\boldsymbol{r}_{i,F}^H+\boldsymbol{r}_{i,F}\right)=\boldsymbol{v}_{i,F}^1+\boldsymbol{v}_{i,F}^2+\boldsymbol{v}_{i,F}^3,\\ \boldsymbol{v}_{i,F}^H&=\widetilde{\boldsymbol{u}}_{i,F}^H+\left(\boldsymbol{\Psi}_{i,F}^H+\boldsymbol{\Psi}_{i,\partial F}^H\right)+\boldsymbol{r}_{i,F}^H=\boldsymbol{v}_{i,F}^{1,H}+\boldsymbol{v}_{i,F}^{2,H}+\boldsymbol{v}_{i,F}^{3,H},\end{aligned} \tag{4.11}$$

with the conditions

$$\begin{cases}\lambda_f\left(\boldsymbol{v}_{i,F}^j\right)=\lambda_f\left(\boldsymbol{u}_i^j\right), & \lambda_f\left(\boldsymbol{v}_{i,F}^{j,H}\right)=\lambda_f\left(\rho_H^{RT}\boldsymbol{u}_i^j\right) & \text{if } f\subset F,\\ \lambda_f\left(\boldsymbol{v}_{i,F}^j\right)=0, & \lambda_f\left(\boldsymbol{v}_{i,F}^{j,H}\right)=0 & \text{if } f\subset \partial\Omega_i\backslash F,\end{cases} \tag{4.12}$$

and

$$a_i\left(\boldsymbol{v}_{i,F}^j-\boldsymbol{v}_{i,F}^{j,H},\boldsymbol{v}_{i,F}^j-\boldsymbol{v}_{i,F}^{j,H}\right)\leq C\left(1+\log H_i/h_i\right)^2 a_i\left(\boldsymbol{u}_i,\boldsymbol{u}_i\right) \tag{4.13}$$

for $j=1,2,3$. Here, $\boldsymbol{r}_i^H:=\rho_H^{RT}\left(\mathbf{curl}\,\boldsymbol{q}_i\right)$, $r_i:=\left(\mathbf{curl}\,\boldsymbol{q}_i\right)\cdot\boldsymbol{n}$, and $r_i^H:=\boldsymbol{r}_i^H\cdot\boldsymbol{n}$ and that $\boldsymbol{r}_{i,F}^H:=\mathcal{H}_i\left(\zeta_F r_i^H\right)$ and $\boldsymbol{r}_{i,F}:=\mathcal{H}_i\left(\zeta_F\left(r_i-r_i^H\right)\right)$.

If such $\boldsymbol{v}_{i,F}$ and $\boldsymbol{v}_{i,F}^H$ are available, we can easily prove that the functions satisfy conditions (4.7), (4.8), and (4.9).

Term $\widetilde{\boldsymbol{u}}_i$: We first consider $\widetilde{\boldsymbol{u}}_i$. We define $\widetilde{\boldsymbol{u}}_{i,F}:=\sum_{f\subset F}\lambda_f\left(\widetilde{\boldsymbol{u}}_i\right)\boldsymbol{\phi}_f^{RT}$, where $\boldsymbol{\phi}_f^{RT}$ is the Raviart-Thomas basis function associated with the face f. By using Lemmas 2.2, 2.3, and 4.7, we have

$$\left\|\widetilde{\boldsymbol{u}}_{i,F}\right\|_{0;\Omega_i}^2\leq C\sum_{f\subset F}h_f^3\lambda_f\left(\widetilde{\boldsymbol{u}}_i\right)^2\leq C\left\|\widetilde{\boldsymbol{u}}_i\right\|_{0;\Omega_i}^2\leq Ch_i^2\left\|\operatorname{div}\boldsymbol{u}_i\right\|_{0;\Omega_i}^2\leq C\left\|\boldsymbol{u}_i\right\|_{0;\Omega_i}^2 \tag{4.14}$$

and

$$\left\|\operatorname{div}\widetilde{\boldsymbol{u}}_{i,F}\right\|_{0;\Omega_i}^2\leq C\sum_{f\subset F}h_f\lambda_f\left(\widetilde{\boldsymbol{u}}_i\right)^2\leq C\left\|h_i^{-1}\widetilde{\boldsymbol{u}}_i\right\|_{0;\Omega_i}^2\leq C\left\|\operatorname{div}\boldsymbol{u}_i\right\|_{0;\Omega_i}^2. \tag{4.15}$$

Hence, from (4.14) and (4.15),

$$a_i\left(\widetilde{\boldsymbol{u}}_{i,F},\widetilde{\boldsymbol{u}}_{i,F}\right)\leq Ca_i\left(\boldsymbol{u}_i,\boldsymbol{u}_i\right). \tag{4.16}$$

We also define $\widetilde{\boldsymbol{u}}_{i,F}^H:=\mathcal{H}_i\left(\rho_H^{RT}\widetilde{\boldsymbol{u}}_{i,F}\cdot\boldsymbol{n}\right)$. By using Lemma 4.5 and (4.16), we obtain

$$a_i\left(\widetilde{\boldsymbol{u}}_{i,F}^H,\widetilde{\boldsymbol{u}}_{i,F}^H\right)\leq Ca_i(\widetilde{\boldsymbol{u}}_{i,F},\widetilde{\boldsymbol{u}}_{i,F})\leq Ca_i\left(\boldsymbol{u}_i,\boldsymbol{u}_i\right). \tag{4.17}$$

We note that by construction, $\widetilde{\boldsymbol{u}}_{i,F} - \widetilde{\boldsymbol{u}}_{i,F}^H$ satisfies the no-net-flux condition. We have similarly constructed pairs of functions originating from the other terms of the right-hand side of (4.10) such that their differences satisfy the no-net-flux condition. We only have to note that these three differences all belong to the range of the operator $I - \rho_H^{RT}$.

Term $\rho_h^{RT}(\boldsymbol{\Psi}_i)$: We next consider the second term $\rho_h^{RT}(\boldsymbol{\Psi}_i)$ of (4.10). Let $\boldsymbol{\Psi}_{i,F} := I_h(\vartheta_F \boldsymbol{\Psi}_i)$. By using Lemma 2.5 and Lemma 2.6, we obtain

$$\left\|\rho_h^{RT}(\boldsymbol{\Psi}_{i,F})\right\|_{0;\Omega_i}^2 \leq C \left\|\boldsymbol{\Psi}_{i,F}\right\|_{0;\Omega_i}^2 \tag{4.18}$$

and

$$\left\|\operatorname{div} \rho_h^{RT}(\boldsymbol{\Psi}_{i,F})\right\|_{0;\Omega_i}^2 = \left\|\Pi_h(\operatorname{div} \boldsymbol{\Psi}_{i,F})\right\|_{0;\Omega_i}^2 \leq \left\|\operatorname{div} \boldsymbol{\Psi}_{i,F}\right\|_{0;\Omega_i}^2. \tag{4.19}$$

Moreover, by using Lemmas 4.1 and 4.7, we obtain

$$\left\|\boldsymbol{\Psi}_{i,F}\right\|_{0;\Omega_i}^2 \leq C \left\|\boldsymbol{\Psi}_i\right\|_{0;\Omega_i}^2 \leq C \left\|\boldsymbol{u}_i\right\|_{0;\Omega_i}^2 \tag{4.20}$$

and

$$\begin{aligned} \left\|\operatorname{div} \boldsymbol{\Psi}_{i,F}\right\|_{0;\Omega_i}^2 &\leq C \left|\boldsymbol{\Psi}_{i,F}\right|_{1;\Omega_i}^2 \leq C \left(1 + \log H_i/h_i\right)^2 \left\|\boldsymbol{\Psi}_i\right\|_{1;\Omega_i}^2 \\ &\leq C \left(1 + \log H_i/h_i\right)^2 \left\|\operatorname{div} \boldsymbol{u}_i\right\|_{0;\Omega_i}^2. \end{aligned} \tag{4.21}$$

Therefore, from (4.18), (4.19), (4.20) and (4.21), we have

$$\left\|\rho_h^{RT}(\boldsymbol{\Psi}_{i,F})\right\|_{0;\Omega_i}^2 \leq C \left\|\boldsymbol{u}_i\right\|_{0;\Omega_i}^2 \tag{4.22}$$

and

$$\left\|\operatorname{div} \rho_h^{RT}(\boldsymbol{\Psi}_{i,F})\right\|_{0;\Omega_i}^2 \leq C \left(1 + \log H_i/h_i\right)^2 \left\|\operatorname{div} \boldsymbol{u}_i\right\|_{0;\Omega_i}^2. \tag{4.23}$$

Hence, from (4.22) and (4.23), we obtain

$$a_i\left(\rho_h^{RT}(\boldsymbol{\Psi}_{i,F}), \rho_h^{RT}(\boldsymbol{\Psi}_{i,F})\right) \leq C \left(1 + \log H_i/h_i\right)^2 a_i(\boldsymbol{u}_i, \boldsymbol{u}_i). \tag{4.24}$$

Let $\boldsymbol{\Psi}_{i,F}^H := \mathcal{H}_i\left(\rho_H^{RT}\left(\rho_h^{RT} \boldsymbol{\Psi}_{i,F}\right) \cdot \boldsymbol{n}\right)$. By using Lemma 4.5 and (4.24), we have

$$\begin{aligned} a_i\left(\boldsymbol{\Psi}_{i,F}^H, \boldsymbol{\Psi}_{i,F}^H\right) &\leq C a_i\left(\rho_h^{RT}(\boldsymbol{\Psi}_{i,F}), \rho_h^{RT}(\boldsymbol{\Psi}_{i,F})\right) \\ &\leq C \left(1 + \log H_i/h_i\right)^2 a_i(\boldsymbol{u}_i, \boldsymbol{u}_i). \end{aligned} \tag{4.25}$$

Let $\boldsymbol{g}_{i,\partial F} := \rho_h^{RT}(I_h(\vartheta_{\partial F} \boldsymbol{\Psi}_i))$ and $\boldsymbol{\Psi}_{i,\partial F} := \sum_{f \subset F} \lambda_f(\boldsymbol{g}_{i,\partial F}) \boldsymbol{\phi}_f^{RT}$. By using Lemmas 2.2, 2.5, 4.1, and 4.7, and an estimate for the P_1 basis functions of $S(\Omega_i)$, we obtain

$$\begin{aligned} \left\|\boldsymbol{\Psi}_{i,\partial F}\right\|_{0;\Omega_i}^2 &\leq C \sum_{f \subset F} h_f^3 \lambda_f(\boldsymbol{g}_{i,\partial F})^2 \leq C \left\|\boldsymbol{g}_{i,\partial F}\right\|_{0;\Omega_i}^2 \\ &\leq C \left\|I_h(\vartheta_{\partial F} \boldsymbol{\Psi}_i)\right\|_{0;\Omega_i}^2 \leq C \left\|\boldsymbol{\Psi}_i\right\|_{0;\Omega_i}^2 \leq C \left\|\boldsymbol{u}_i\right\|_{0;\Omega_i}^2 \end{aligned} \tag{4.26}$$

and

$$\begin{aligned} \left\|\operatorname{div} \boldsymbol{\Psi}_{i,\partial F}\right\|_{0;\Omega_i}^2 &\leq C \sum_{f \subset F} h_f \lambda_f(\boldsymbol{g}_{i,\partial F})^2 \leq C \frac{1}{h_i^2} \left\|\boldsymbol{g}_{i,\partial F}\right\|_{0;\Omega_i}^2 \leq C \frac{1}{h_i^2} \left\|I_h(\vartheta_{\partial F} \boldsymbol{\Psi}_i)\right\|_{0;\Omega_i}^2 \\ &\leq C \left\|\boldsymbol{\Psi}_i\right\|_{0;\partial F}^2 \leq C \left(1 + \log H_i/h_i\right) \left\|\boldsymbol{\Psi}_i\right\|_{1;\Omega_i}^2 \\ &\leq C \left(1 + \log H_i/h_i\right) \left\|\operatorname{div} \boldsymbol{u}_i\right\|_{0;\Omega_i}^2. \end{aligned} \tag{4.27}$$

Hence, combining (4.26) and (4.27), we obtain

$$a_i\left(\boldsymbol{\Psi}_{i,\partial F},\boldsymbol{\Psi}_{i,\partial F}\right)\leq C\left(1+\log H_i/h_i\right)a_i\left(\boldsymbol{u}_i,\boldsymbol{u}_i\right). \tag{4.28}$$

Let $\boldsymbol{\Psi}^H_{i,\partial F}:=\mathcal{H}_i\left(\rho^{RT}_H\boldsymbol{\Psi}_{i,\partial F}\cdot\boldsymbol{n}\right)$. From Lemma 4.5 and (4.28), we obtain

$$\begin{aligned}a_i\left(\boldsymbol{\Psi}^H_{i,\partial F},\boldsymbol{\Psi}^H_{i,\partial F}\right)&\leq Ca_i\left(\boldsymbol{\Psi}_{i,\partial F},\boldsymbol{\Psi}_{i,\partial F}\right)\\&\leq C\left(1+\log H_i/h_i\right)a_i\left(\boldsymbol{u}_i,\boldsymbol{u}_i\right).\end{aligned} \tag{4.29}$$

Term $\mathbf{curl}\,\boldsymbol{q}_i$: We finally consider the $\mathbf{curl}\,\boldsymbol{q}_i$ term of (4.10). Recall that $\boldsymbol{r}^H_i:=\rho^{RT}_H\left(\mathbf{curl}\,\boldsymbol{q}_i\right)$, $r_i:=\left(\mathbf{curl}\,\boldsymbol{q}_i\right)\cdot\boldsymbol{n}$, and $r^H_i:=\boldsymbol{r}^H_i\cdot\boldsymbol{n}$ and that $\boldsymbol{r}^H_{i,F}:=\mathcal{H}_i\left(\zeta_F r^H_i\right)$ and $\boldsymbol{r}_{i,F}:=\mathcal{H}_i\left(\zeta_F\left(r_i-r^H_i\right)\right)$.

From Corollary 4.3 and Lemma 4.6, we obtain

$$\begin{aligned}&a_i\left(\boldsymbol{r}_{i,F},\boldsymbol{r}_{i,F}\right)\\&\leq C\beta_i\left\|\zeta_F\left(r_i-r^H_i\right)\right\|^2_{-1/2;\partial\Omega_i}\\&\leq C\beta_i\left(1+\log H_i/h_i\right)\left(\left(1+\log H_i/h_i\right)\left\|r_i\right\|^2_{-1/2;\partial\Omega_i}+\left\|r_i-r^H_i\right\|^2_{-1/2;\partial\Omega_i}\right)\\&\leq C\beta_i\left(1+\log H_i/h_i\right)\left(\left(1+\log H_i/h_i\right)\left\|r_i\right\|^2_{-1/2;\partial\Omega_i}+\left\|r^H_i\right\|^2_{-1/2;\partial\Omega_i}\right)\\&=C\beta_i\left(1+\log H_i/h_i\right)^2\left\|r_i\right\|^2_{-1/2;\partial\Omega_i}+C\beta_i\left(1+\log H_i/h_i\right)\left\|r^H_i\right\|^2_{-1/2;\partial\Omega_i}.\end{aligned} \tag{4.30}$$

We note that $\left\|\mathrm{div}\,\boldsymbol{r}^H_i\right\|_{0;\Omega_i}\leq\left\|\mathrm{div}\left(\mathbf{curl}\,\boldsymbol{q}_i\right)\right\|_{0;\Omega_i}=0$ from Lemma 4.4. Hence, by using Lemmas 2.1 and 4.4, we obtain

$$\begin{aligned}\left\|r^H_i\right\|^2_{-1/2;\partial\Omega_i}&\leq C\left(H_i^2\left\|\mathrm{div}\,\boldsymbol{r}^H_i\right\|^2_{0;\Omega_i}+\left\|\boldsymbol{r}^H_i\right\|^2_{0;\Omega_i}\right)=C\left\|\boldsymbol{r}^H_i\right\|^2_{0;\Omega_i}\\&\leq C\left(\left(1+\log H_i/h_i\right)\left\|\mathbf{curl}\,\boldsymbol{q}_i\right\|^2_{0;\Omega_i}+H_i^2\left\|\mathrm{div}\left(\mathbf{curl}\,\boldsymbol{q}_i\right)\right\|^2_{0;\Omega_i}\right)\\&=C\left(1+\log H_i/h_i\right)\left\|\mathbf{curl}\,\boldsymbol{q}_i\right\|^2_{0;\Omega_i}\end{aligned} \tag{4.31}$$

and

$$\begin{aligned}\left\|r_i\right\|^2_{-1/2;\partial\Omega_i}&\leq C\left(H_i^2\left\|\mathrm{div}\left(\mathbf{curl}\,\boldsymbol{q}_i\right)\right\|^2_{0;\Omega_i}+\left\|\mathbf{curl}\,\boldsymbol{q}_i\right\|^2_{0;\Omega_i}\right)\\&=C\left\|\mathbf{curl}\,\boldsymbol{q}_i\right\|^2_{0;\Omega_i}.\end{aligned} \tag{4.32}$$

Therefore, by combining (4.30), (4.31), (4.32), and Lemma 4.7, we obtain

$$\begin{aligned}a_i\left(\boldsymbol{r}_{i,F},\boldsymbol{r}_{i,F}\right)&\leq C\left(1+\log H_i/h_i\right)^2\beta_i\left\|\mathbf{curl}\,\boldsymbol{q}_i\right\|^2_{0;\Omega_i}\\&\leq C\left(1+\log H_i/h_i\right)^2\beta_i\left\|\boldsymbol{u}_i\right\|^2_{0;\Omega_i}\\&\leq C\left(1+\log H_i/h_i\right)^2a_i\left(\boldsymbol{u}_i,\boldsymbol{u}_i\right).\end{aligned} \tag{4.33}$$

Then, $\boldsymbol{v}_{i,F}$ and $\boldsymbol{v}^H_{i,F}$ satisfy the conditions (4.7) and (4.8), respectively. Furthermore, we obtain the following estimate by using (4.16), (4.17), (4.24), (4.25), (4.28), (4.29), and (4.33):

$$a_i\left(\boldsymbol{v}_{i,F}-\boldsymbol{v}^H_{i,F},\boldsymbol{v}_{i,F}-\boldsymbol{v}^H_{i,F}\right)\leq C\left(1+\log H_i/h_i\right)^2a_i\left(\boldsymbol{u}_i,\boldsymbol{u}_i\right). \qquad \square$$

By using Lemma 4.8, we have now arrived at our main theoretical result.

Theorem 4.9 (Condition number estimate)**.** *Let each subdomain be convex and a union of a finite number of coarse elements, let the triangulation of each subdomain be quasi-uniform and assume that material parameters are constant in each subdomain. Then, the condition number of the preconditioned operator $M^{-1}\widehat{S}_\Gamma$ satisfies*

$$\kappa\left(M^{-1}\widehat{S}_\Gamma\right) \leq C\left(1+\log H/h\right)^2, \tag{4.34}$$

where C is independent of α, β, h, and H.

5. Numerical results

All results in this section, except when otherwise stated, are for problems on the domain $\Omega = [0,1]^3$ and for a two-level BDDC algorithm. The triangulation of Ω and the assembly of the subdomain matrices are performed using the C++ library DOLFIN [53], which is part of the FEniCS project [52]. ParMETIS [37] is used to decompose the meshes and always results in irregular subdomains.

The linear system (3.2) is solved using the Preconditioned Conjugate Gradient (PCG) method as implemented in the Portable and Extensible Toolbox for Scientific Computing (PETSc) [9] with the BDDC preconditioner implemented in PETSc by the third author (see [89]) for which each subdomain is assigned to a different MPI process. The right-hand sides are always chosen randomly, the initial guess as zero, and a relative reduction of the Euclidean norm of the residual of 10^{-8} is used as a stopping criterion.

The MUMPS [2] Cholesky factorizations are used for the subdomain solvers and to compute the local Schur complements. The current PETSc implementation uses dense linear algebra kernels (see [3]) for solving (3.11) for each subdomain face, and the small dense blocks $S_{FF}^{(i)}$ are inverted explicitly. Formula (3.10) is not used in practice; instead, each $S_\Gamma^{(i)}$ is first explicitly inverted, and the principal minors $\breve{S}_{FF}^{(i)-1}$ are then extracted. We always ignore the overly pessimistic factor N_F^2, as given by Theorem 3.3, for the specification of the eigenvalue threshold of (3.11). Our experience has shown that the condition number consistently will be close to our choice of ν_{tol}.

Unless otherwise stated, we use the averages of the normal component over each subdomain face as our primal constraints as provided by the no-net-flux condition. The quadrature weights for these constraints can easily be obtained by using the divergence theorem, i.e.,

$$\int_{\Gamma_i} \boldsymbol{u}\cdot\boldsymbol{n} = \int_{\Omega_i} \operatorname{div}\boldsymbol{u}.$$

Our large scale numerical results have been obtained on the Cray XC40 Shaheen of KAUST, ranked 10th in the Top500 list as of June 2016, and which features 6192 dual 16-core Haswell processors clocked at 2.3 Ghz and equipped with 128GB of DRAM per node, for a total of 198,144 cores. For further details on the BDDC implementation and for additional numerical results for our $H(\mathrm{div})$ model problem, see [89].

Of our examples, only the final one concerns three-level BDDC.

TABLE 1. Condition numbers (κ_2) and iteration counts (it) for the lowest order Raviart-Thomas elements with different mesh sizes. $\alpha_i = \alpha_o = 1$ for odd subdomains and $\alpha_i = \alpha_e$ for even subdomains, $\beta_i \equiv 1$; there are 64 irregular subdomains.

	$H/h = 4.3$		$H/h = 7.3$		$H/h = 11.1$		$H/h = 13.5$	
	κ_2	it	κ_2	it	κ_2	it	κ_2	it
$\alpha_e = 10^{-2}$	3.15	13	3.67	14	4.38	15	5.17	16
$\alpha_e = 10^{-1}$	3.53	14	4.31	15	4.92	16	5.21	16
$\alpha_e = 10^{0}$	3.84	15	4.52	15	5.69	17	5.57	16
$\alpha_e = 10^{1}$	3.90	14	4.56	14	5.87	16	5.68	16
$\alpha_e = 10^{2}$	3.91	13	4.57	13	5.89	15	5.70	16

TABLE 2. Condition numbers (κ_2) and iteration counts (it) for the lowest order Raviart-Thomas elements with different mesh sizes. $\beta_i = \beta_o = 1$ for odd subdomains and $\beta_i = \beta_e$ for even subdomains, $\alpha_i \equiv 1$; there are 64 irregular subdomains.

	$H/h = 4.3$		$H/h = 7.3$		$H/h = 11.1$		$H/h = 13.5$	
	κ_2	it	κ_2	it	κ_2	it	κ_2	it
$\beta_e = 10^{-2}$	4.77	14	5.10	15	6.05	17	6.66	17
$\beta_e = 10^{-1}$	4.62	14	4.91	15	5.74	16	5.96	17
$\beta_e = 10^{0}$	3.84	15	4.52	15	5.69	17	5.57	16
$\beta_e = 10^{1}$	4.67	15	5.09	15	5.29	17	5.02	16
$\beta_e = 10^{2}$	5.02	15	5.68	16	5.96	18	5.56	17

5.1. **Example 1 (Common average constraints).** We decompose the unit cube Ω into 64 irregular subdomains using ParMETIS and assume that the coefficients α and β have jumps only across the interface between the subdomains. We have conducted two different sets of experiments for the lowest order Raviart-Thomas and BDM elements. For the first set of experiments, we report on the condition numbers and the number of iterations for different values of H/h, with a constant value of β while varying α between the subdomains. Here and in what follows, H/h is defined as the maximum of the ratio of the diameter of a subdomain and the smallest diameter of any of its elements. The subdomains are subdivided into even and odd subdomains according to their MPI rank. In the second set of experiments, the value of α is constant while β varies. As predicted by the theory, the experimental results in Tables 1 and 2 confirm that the condition number of deluxe BDDC is insensitive to the jumps of the coefficients for the lowest order Raviart-Thomas elements. As indicated by the results in Tables 3 and 4, the no-net-flux condition is also sufficient to obtain condition number independence for the lowest order BDM elements.

5.2. **Example 2 (The effect of using conventional averaging techniques).** In this subsection, we report on some numerical experiments comparing deluxe BDDC and conventional scaling techniques. We have performed four different types of experiments with the same set of coefficient distributions using the lowest order Raviart-Thomas and BDM elements. The first set of experiments, named "deluxe",

TABLE 3. Condition numbers (κ_2) and iteration counts (it) for the lowest order BDM elements with different mesh sizes. $\alpha_i = \alpha_o = 1$ for odd subdomains and $\alpha_i = \alpha_e$ for even subdomains, $\beta_i \equiv 1$; there are 64 irregular subdomains.

	$H/h = 4.3$		$H/h = 7.3$		$H/h = 11.1$		$H/h = 13.5$	
	κ_2	it	κ_2	it	κ_2	it	κ_2	it
$\alpha_e = 10^{-2}$	5.04	17	6.38	19	6.59	19	7.91	20
$\alpha_e = 10^{-1}$	5.99	19	6.84	20	7.59	21	7.97	21
$\alpha_e = 10^{0}$	6.49	20	7.18	20	8.69	21	8.44	21
$\alpha_e = 10^{1}$	6.59	19	7.24	19	8.96	21	8.59	20
$\alpha_e = 10^{2}$	6.60	18	7.25	18	9.00	19	8.62	19

TABLE 4. Condition numbers (κ_2) and iteration counts (it) for the lowest order BDM elements with different mesh sizes. $\beta_i = \beta_o = 1$ for odd subdomains and $\beta_i = \beta_e$ for even subdomains, $\alpha_i \equiv 1$; there are 64 irregular subdomains.

	$H/h = 4.3$		$H/h = 7.3$		$H/h = 11.1$		$H/h = 13.5$	
	κ_2	it	κ_2	it	κ_2	it	κ_2	it
$\beta_e = 10^{-2}$	7.99	19	8.61	20	10.25	22	11.80	23
$\beta_e = 10^{-1}$	7.39	20	7.75	19	9.04	21	9.11	22
$\beta_e = 10^{0}$	6.49	20	7.18	20	8.69	21	8.44	21
$\beta_e = 10^{1}$	6.96	21	7.85	20	8.13	22	8.26	21
$\beta_e = 10^{2}$	8.51	21	8.87	22	9.45	24	10.32	23

is based on the weighted averaging techniques as described in (3.9). In the second, the economic variant of the deluxe scaling ("e-deluxe") is used with one layer of elements next to Γ. The results in the third and fourth columns of Tables 5 and 6 are obtained by using conventional methods as described in [21, 56]. In the "stiffness" case, the scaling is based on the diagonal entries of the subdomain matrices, whereas in the "card" case, we use the usual cardinality scaling, which for Raviart-Thomas elements and BDM elements results in using 1/2 as the scaling factor for each interface degree of freedom. For other general settings, we follow subsection 5.1. As we see in Tables 5 and 6, our weighted averaging technique, even in its economic version, works well for both Raviart-Thomas elements and BDM elements, while the other scaling choices are sensitive to discontinuities across the interface.

5.3. **Example 3 (Using higher order elements).** In this subsection, we report on the dependence of the rate of convergence of the deluxe BDDC algorithm on the polynomial order of the finite element spaces. We recall that our theory does not cover such cases. We consider a constant coefficient case, i.e., $\alpha = \beta = 1$, and fix the fine triangulation of Ω. We then increase the polynomial order for the Raviart-Thomas elements and BDM elements; the order of the lowest order elements is equal to 1. The experimental condition numbers for Raviart-Thomas (continuous line) and for BDM (dashed line), as reported in Figure 1, indicate a polylogarithmic bound in the polynomial order of the finite element spaces as observed and theoretically justified for a spectral element case in [65].

TABLE 5. Condition numbers (κ_2) and iteration counts (it) for the lowest order Raviart-Thomas elements with different scalings. $\alpha_i = \alpha_o = 1$ and $\beta_i = \beta_o = 1$ for the odd subdomains and $\alpha_i = \alpha_e$ and $\beta_i = \beta_e$ for even subdomains, 64 irregular subdomains, and $H/h = 7.3$.

	deluxe		e-deluxe		stiffness		card	
	κ_2	it	κ_2	it	κ_2	it	κ_2	it
$\alpha_e = 10^{-2}$, $\beta_e = 10^{2}$	4.71	15	4.67	15	1.8e2	97	5.1e1	57
$\alpha_e = 10^{-1}$, $\beta_e = 10^{1}$	4.05	15	4.02	15	7.3e1	63	2.2e1	35
$\alpha_e = 10^{0}$, $\beta_e = 10^{0}$	4.52	15	4.48	15	5.3e0	17	5.3e0	16
$\alpha_e = 10^{1}$, $\beta_e = 10^{-1}$	4.52	14	4.24	14	1.1e2	64	3.4e1	36
$\alpha_e = 10^{2}$, $\beta_e = 10^{-2}$	5.11	14	4.52	14	1.2e3	158	3.2e2	101

TABLE 6. Condition numbers (κ_2) and iteration counts (it) for the lowest order BDM elements with different scalings. $\alpha_i = \alpha_o = 1$ and $\beta_i = \beta_o = 1$ for the odd subdomains and $\alpha_i = \alpha_e$ and $\beta_i = \beta_e$ for even subdomains, 64 irregular subdomains, and $H/h = 7.3$.

	deluxe		e-deluxe		stiffness		card	
	κ_2	it	κ_2	it	κ_2	it	κ_2	it
$\alpha_e = 10^{-2}$, $\beta_e = 10^{2}$	8.66	21	8.30	21	2.1e2	119	1.6e2	95
$\alpha_e = 10^{-1}$, $\beta_e = 10^{1}$	6.89	20	6.60	20	1.1e2	81	3.8e1	48
$\alpha_e = 10^{0}$, $\beta_e = 10^{0}$	7.18	20	7.15	20	7.8e0	21	7.8e0	21
$\alpha_e = 10^{1}$, $\beta_e = 10^{-1}$	7.41	20	6.85	20	1.6e2	83	5.1e1	47
$\alpha_e = 10^{2}$, $\beta_e = 10^{-2}$	8.61	20	7.81	20	1.8e3	235	4.8e2	131

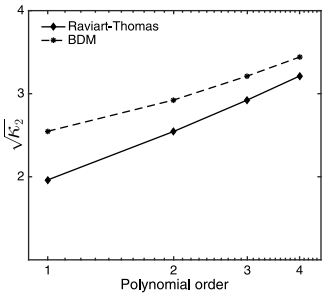

FIGURE 1. Square root of condition numbers as a function of logarithm of the polynomial order for Raviart-Thomas (continuous line) and BDM (dashed line) elements. $\alpha = \beta = 1$, with 64 irregular subdomains and $H/h = 4.3$.

5.4. **Example 4 (Adaptive BDDC deluxe).** In this subsection, we report on the efficiency of adaptive BDDC deluxe, and its economic variant, with randomly distributed material coefficients α and β, using $\nu_{tol} = 10$ for the eigenvalue problem (3.11) ignoring the factor N_F^2 of Theorem 3.3. We consider different refinements of $\Omega = [0,1]^3$ which is always decomposed into 64 irregular subdomains. For the material coefficient α (resp. β), we first draw a set of random real numbers $x_\alpha \in$

TABLE 7. Condition numbers (κ_2), iteration counts (it), and relative size, in percent, of primal spaces (Π) for the lowest order Raviart-Thomas elements with randomly chosen coefficients $\alpha, \beta \in [10^{-q}, 10^{q}]$, with 64 irregular subdomains. Adaptive BDDC with $\nu_{tol} = 10$. Results given for deluxe and e-deluxe versions.

	$q=1$			$q=2$			$q=3$			$q=4$		
	κ_2	it	Π	κ_2	it	Π	κ_2	it	Π	κ_2	it	Π
H/h	deluxe											
8.1	10.9	22	6.1	8.1	20	11.9	10.6	21	14.9	10.5	20	15.0
16.2	11.2	23	1.6	9.2	21	4.9	12.1	21	7.3	11.6	20	7.9
22.4	11.3	23	0.8	11.5	21	3.3	9.9	19	5.2	10.9	19	5.9
30.5	11.1	23	0.5	11.9	21	2.4	11.5	20	3.8	13.1	20	4.4
34.9	10.5	22	0.3	11.6	20	1.9	13.9	20	3.2	11.8	18	3.7
40.8	11.7	22	0.2	10.0	19	1.6	12.4	21	2.6	11.2	18	3.1
H/h	e-deluxe											
8.1	10.9	22	6.2	8.2	20	11.9	10.6	21	15.0	10.5	20	15.1
16.2	11.2	23	1.7	9.2	21	5.0	12.1	21	7.3	11.7	20	8.0
22.4	11.3	23	0.9	11.3	21	3.4	9.7	19	5.3	10.9	19	6.0
30.5	11.1	20	0.6	11.7	20	2.5	11.3	20	3.9	13.1	20	4.5
34.9	9.5	21	0.4	9.7	19	2.0	13.5	20	3.3	11.5	18	3.8
40.8	11.6	22	0.3	9.8	19	1.7	12.1	20	2.7	11.1	18	3.2

$[-q, q]$ ($x_\beta \in [-q, q]$) and then set $\alpha = 10^{x_\alpha}$ ($\beta = 10^{x_\beta}$). Results for the lowest order Raviart-Thomas discretization are given in Table 7; as the mesh is refined, the number of degrees of freedom increases from 50 thousand ($H/h = 8.1$) to 10 million ($H/h = 40.8$). Similar results for the lowest order BDM elements are provided in Table 8; the number of degrees of freedom varies from 152 thousand ($H/h = 8.1$) to 9 million ($H/h = 30.5$). Larger values of H/h for BDM discretization were not possible because of memory issues related with the local factorizations. The condition numbers, the number of iterations, and the size of the adaptive primal spaces, given as a percentage of the number of degrees of freedom on the interface, are provided. H/h is increased from top to bottom, whereas the contrast in the coefficients is increased from left to right. We stress that the random distributions considered for α and β are different.

Experimental condition numbers are very close to the adaptive threshold used in all the deluxe and e-deluxe adaptive BDDC runs; the size of the adaptively generated coarse problems are very similar, with the e-deluxe version always producing slightly larger primal spaces. These numerical results, together with the observation that the relative size of the primal spaces always decreases as H/h increases, support our adaptive theory (see Theorem 3.3), and indicate that the large eigenvalues of the preconditioned spectrum are only linked to the behavior of the coefficients close to the interface. It is also interesting to note that the relative size of the adaptively generated primal spaces for BDM discretization is smaller, being roughly a third of those generated with Raviart-Thomas elements.

Figure 2 shows the timings for the setup and the application of the adaptive BDDC preconditioner for the lowest order Raviart-Thomas elements. We compare

TABLE 8. Condition numbers (κ_2), iteration counts (it), and relative size, in percent, of primal spaces (Π) for the lowest order BDM elements with randomly chosen coefficients $\alpha, \beta \in [10^{-q}, 10^{q}]$, with 64 irregular subdomains. Adaptive BDDC with $\nu_{tol} = 10$. Results given for deluxe and e-deluxe versions.

	$q=1$			$q=2$			$q=3$			$q=4$		
	κ_2	it	Π	κ_2	it	Π	κ_2	it	Π	κ_2	it	Π
H/h	deluxe											
8.1	9.0	23	2.3	7.1	20	4.3	11.2	21	4.4	10.3	21	5.3
16.2	10.9	23	0.7	9.3	21	1.8	13.0	22	1.8	9.3	19	2.5
22.4	10.6	22	0.4	11.4	20	1.2	10.8	20	1.2	9.7	19	1.8
30.5	10.4	22	0.2	10.5	21	0.9	11.4	21	0.9	11.9	20	1.3
H/h	e-deluxe											
8.1	9.1	23	2.3	7.1	20	4.3	11.1	21	4.4	10.3	21	5.3
16.2	10.9	23	0.7	9.3	21	1.8	13.0	22	1.8	9.3	19	2.6
22.4	10.5	22	0.4	11.2	20	1.2	10.7	20	1.2	9.7	19	1.8
30.5	9.8	21	0.3	10.4	21	0.9	11.4	20	0.9	11.7	20	1.3

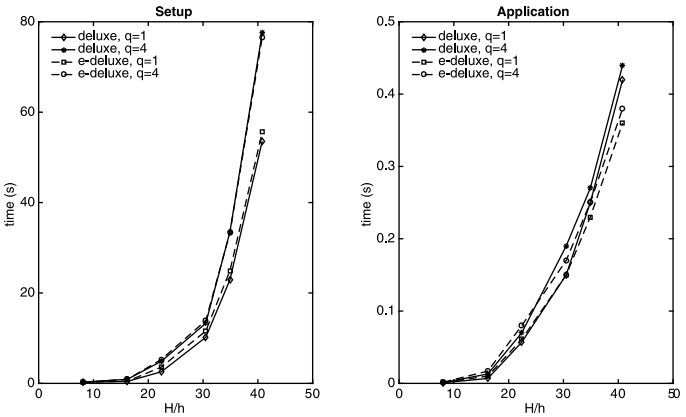

FIGURE 2. Setup times (left) and times for the application of the adaptive BDDC preconditioner (right) as a function of H/h. Deluxe scaling compared against e-deluxe for different values of q, with α and β randomly chosen in $[10^{-q}, 10^{q}]$.

deluxe (continuous line) and e-deluxe (dashed line) for the cases $q = 1$ and $q = 4$. Setup times are comparable for deluxe and e-deluxe, with the former being slightly faster. On the other hand, e-deluxe is asymptotically faster than standard deluxe for larger values of H/h with respect to the solve times.

In the e-deluxe case, the Dirichlet and Neumann solvers are factored separately. These matrices are quite sparse with at most 7 nonzeros per row; in our experience the factorization, and the backward and forward substitution steps are very fast. Instead, in the deluxe case, one single factorization step with the Schur complement computation is performed. This results in a different ordering of the unknowns (provided by MUMPS) and a larger number of nonzeros in the sparse factors for

TABLE 9. Condition numbers (κ_2) and iteration counts (it) for SPE10 test case for different number N of subdomains. Setup time for adaptive BDDC and total time for Krylov solver are shown (in seconds); in parenthesis, the speed-up in relation to the case of 128 subdomains.

N	κ_2	it	setup	solve	ideal
128	12.6	20	26.51 (1.0)	6.51 (1.0)	1
256	13.1	21	8.91 (2.9)	2.92 (2.2)	2
512	14.0	22	3.83 (6.9)	1.27 (5.1)	4
1024	14.9	22	1.73 (15.3)	0.61 (10.7)	8

the Dirichlet solver. The local Neumann problems are instead solved with a dense matrix-vector multiplication, reusing the Schur complement inverted during the setup phase. Such a step has $O(n_\Gamma^2)$ complexity, where n_Γ is the number of degrees of freedom of the subdomain interface. A poor load balance of the unknowns of the local interfaces impacts the timings of this application negatively; see also [89]. We have observed similar results for the lowest order BDM elements, with about 21 nonzeros per row (data not shown).

5.5. **Example 5 (Strong scalability with an SPE10 test case).** In this subsection, we report on the strong scaling for adaptive deluxe BDDC for a slightly different variational problem given by

$$a(\boldsymbol{u},\boldsymbol{v}) := \int_\Omega (P \operatorname{div} \boldsymbol{u} \operatorname{div} \boldsymbol{v} + \boldsymbol{u}\ K^{-1}\ \boldsymbol{v}) dx, \tag{5.1}$$

where P is a nonnegative scalar and K a symmetric positive definite tensor. The porosity and the tensor permeability coefficients are given by the second data set of the well-known SPE10 benchmark; cf. [1]. The domain considered is 1200ft $\times$ 2200ft $\times$ 170ft, regularly decomposed by a hexahedral grid of $60 \times 220 \times 85$, with each resulting hexahedron further subdivided into 6 tetrahedra. We use the lowest order Raviart-Thomas elements, for a total of 15M degrees of freedom, and consider the effect of increasing the number of subdomains N. We stress that the aspect ratio of the elements is very high for the test case considered.

The porosity field is strongly correlated with the permeability coefficients, which have very large variations (8 to 12 orders of magnitude). About 3% of the elements have zero porosity. We note that we are not working with a discretization of the original reservoir Darcy problem. Instead, we use this variational problem in order to test our adaptive BDDC method on problems with highly irregular coefficients. Adaptive deluxe BDDC is used with a threshold of 10 for the eigenvalues of (3.11); the resulting coarse problem is solved using the parallel Cholesky solver provided by the MUMPS library, [2]. Table 9 shows the results; experimental condition numbers are very close to the eigenvalue threshold used, and the number of iterations is scalable with an increasing number of subdomains. A super-linear speed-up can be observed by inspecting the timings for the setup of the preconditioner (setup column) and the total time for the Krylov solver, indicating that in the regimes considered the computational times are dominated by the local Cholesky solvers used for the sparse subdomain problems and for the dense Schur complement, while the size of the coarse problem does not impact the scalability.

5.6. **Example 6 (Strong scalability test with adaptive three-level BDDC).** In this last subsection, we demonstrate the effectiveness of adaptive three-level BDDC for the model problem (1.1) in a strong scaling setting. For weak scaling results with up to 32,768 processes, see [89]. We consider a uniform mesh of the unit cube which results in about 25 million degrees of freedom for the lowest order Raviart-Thomas discretization, and increase the number of subdomains N, from 1,024 to 16,384. The material parameters are randomly chosen in the range $[10^{-3}, 10^{3}]$ and we set $\nu_{tol} = 10$ for (3.11). Results in Figure 3 compare setup times and Krylov solving times using adaptive BDDC deluxe with a parallel Cholesky coarse solver (exact in the legend) against its three-level variants (CR64 and CR128), where the parallel Cholesky coarse solver is replaced by a second step of adaptive BDDC deluxe. In the CR64 (resp. CR128) case, 64 (128) fine subdomains are aggregated, using ParMETIS, into single coarse subdomains. The threshold for the selection of the primal space at the coarser level is set to 5.

Compared with the SPE10 case studied in the previous subsection, the primal spaces generated in this case are larger (data not shown); the costs for the setup and the application of the parallel coarse solver are no longer negligible, and dominate the simulations for large numbers of subdomains. On the other hand, adaptive three-level BDDC algorithms are still scalable in the number of Krylov iterations, requiring a few more iterations to converge than the standard two-levels BDDC; setup and the solve times for the three-level results are scalable up to 16,384 subdomains.

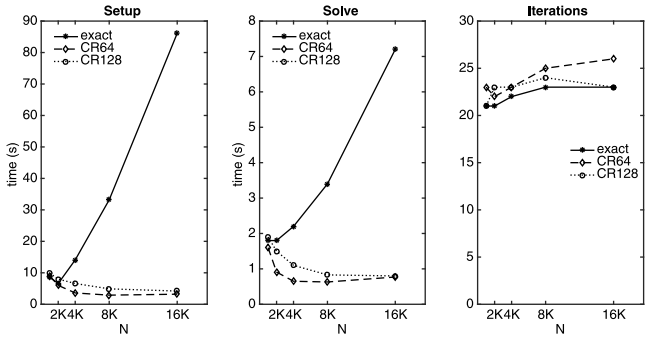

FIGURE 3. Setup (left) and Krylov solver (right) times (in seconds) as a function of N. Adaptive BDDC with eigenvalue threshold $\nu_{tol} = 10$; two-level BDDC with parallel direct coarse solver (exact) compared against three-level BDDC algorithms (CR64 and CR128), with the coarse eigenvalue threshold $\nu_{tol} = 5$. Material coefficients α and β randomly chosen in $[10^{-3}, 10^{3}]$.

ACKNOWLEDGMENTS

The work of the second author was supported in part by the National Science Foundation Grants DMS-1216564 and DMS-1522736.

For computer time, this research used the resources of the Supercomputing Laboratory at King Abdullah University of Science & Technology (KAUST) in Thuwal,

Saudi Arabia. The third author wishes to thank Chris Richardson for his help with the set up of the SPE10 benchmark.

Sandia National Laboratories is a multi-mission laboratory managed and operated by National Technology and Engineering Solutions of Sandia, LLC, a wholly owned subsidiary of Honeywell International, Inc., for the United States Department of Energy's National Nuclear Security Administration under Contract DE-NA0003525.

References

[1] *SPE Comparative Solution Projects*, `http://www.spe.org/web/csp/datasets/set02.htm`.

[2] P. R. Amestoy, I. S. Duff, J.-Y. L'Excellent, and J. Koster, *A fully asynchronous multifrontal solver using distributed dynamic scheduling*, SIAM J. Matrix Anal. Appl. **23** (2001), no. 1, 15–41, DOI 10.1137/S0895479899358194. MR1856597

[3] E. Anderson, Z. Bai, C. Bischof, S. Blackford, J. Demmel, J. Dongarra, J. Du Croz, A. Greenbaum, S. Hammarling, A. McKenney, and D. Sorensen, *LAPACK Users' Guide*, third ed., Society for Industrial and Applied Mathematics, Philadelphia, PA, 1999.

[4] W. N. Anderson Jr. and G. E. Trapp, *Shorted operators. II*, SIAM J. Appl. Math. **28** (1975), 60–71, DOI 10.1137/0128007. MR0356949

[5] W. N. Anderson Jr. and R. J. Duffin, *Series and parallel addition of matrices*, J. Math. Anal. Appl. **26** (1969), 576–594, DOI 10.1016/0022-247X(69)90200-5. MR0242573

[6] D. N. Arnold, R. S. Falk, and R. Winther, *Preconditioning discrete approximations of the Reissner-Mindlin plate model* (English, with English and French summaries), RAIRO Modél. Math. Anal. Numér. **31** (1997), no. 4, 517–557. MR1457459

[7] D. N. Arnold, R. S. Falk, and R. Winther, *Preconditioning in $H(\mathrm{div})$ and applications*, Math. Comp. **66** (1997), no. 219, 957–984, DOI 10.1090/S0025-5718-97-00826-0. MR1401938

[8] D. N. Arnold, R. S. Falk, and R. Winther, *Multigrid in $H(\mathrm{div})$ and $H(\mathrm{curl})$*, Numer. Math. **85** (2000), no. 2, 197–217, DOI 10.1007/PL00005386. MR1754719

[9] S. Balay, S. Abhyankar, M. F. Adams, J. Brown, P. Brune, K. Buschelman, L. Dalcin, V. Eijkhout, W. D. Gropp, D. Kaushik, M. G. Knepley, L. C. McInnes, K. Rupp, B. F. Smith, S. Zampini, and H. Zhang, *PETSc Web page*, `http://www.mcs.anl.gov/petsc`, 2015.

[10] L. Beirão da Veiga, C. Chinosi, C. Lovadina, and L. F. Pavarino, *Robust BDDC preconditioners for Reissner-Mindlin plate bending problems and MITC elements*, SIAM J. Numer. Anal. **47** (2010), no. 6, 4214–4238, DOI 10.1137/080717729. MR2585185

[11] L. Beirão da Veiga, D. Cho, L. F. Pavarino, and S. Scacchi, *BDDC preconditioners for isogeometric analysis*, Math. Models Methods Appl. Sci. **23** (2013), no. 6, 1099–1142, DOI 10.1142/S0218202513500048. MR3037302

[12] L. Beirão da Veiga, L. F. Pavarino, S. Scacchi, O. B. Widlund, and S. Zampini, *Isogeometric BDDC preconditioners with deluxe scaling*, SIAM J. Sci. Comput. **36** (2014), no. 3, A1118–A1139. MR3216651

[13] L. Beirão da Veiga, L. F. Pavarino, S. Scacchi, O. B. Widlund, and S. Zampini, *Adaptive selection of primal constraints for isogeometric BDDC deluxe preconditioners*, SIAM J. Sci. Comput. **39** (2017), no. 1, A281–A302, DOI 10.1137/15M1054675. MR3612901

[14] D. Braess, *Finite elements*, 3rd ed., Cambridge University Press, Cambridge, 2007. Theory, fast solvers, and applications in elasticity theory; Translated from the German by Larry L. Schumaker. MR2322235

[15] S. C. Brenner and L.-Y. Sung, *BDDC and FETI-DP without matrices or vectors*, Comput. Methods Appl. Mech. Engrg. **196** (2007), no. 8, 1429–1435, DOI 10.1016/j.cma.2006.03.012. MR2277027

[16] F. Brezzi and M. Fortin, *Mixed and Hybrid Finite Element Methods*, Springer Series in Computational Mathematics, vol. 15, Springer-Verlag, New York, 1991. MR1115205

[17] Z. Cai, R. Lazarov, T. A. Manteuffel, and S. F. McCormick, *First-order system least squares for second-order partial differential equations. I*, SIAM J. Numer. Anal. **31** (1994), no. 6, 1785–1799, DOI 10.1137/0731091. MR1302685

[18] J. G. Calvo, *A two-level overlapping Schwarz method for $H(\mathrm{curl})$ in two dimensions with irregular subdomains*, Electron. Trans. Numer. Anal. **44** (2015), 497–521. MR3407231

[19] J. G. Calvo, *A BDDC algorithm with deluxe scaling for H(curl) in two dimensions with irregular subdomains*, Math. Comp. **85** (2016), no. 299, 1085–1111, DOI 10.1090/mcom/3028. MR3454359

[20] J. G. Calvo and O. B. Widlund, *An adaptive choice of primal constraints for BDDC domain decomposition algorithms*, Electron. Trans. Numer. Anal. **45** (2016), 524–544. MR3582898

[21] C. R. Dohrmann, *A preconditioner for substructuring based on constrained energy minimization*, SIAM J. Sci. Comput. **25** (2003), no. 1, 246–258, DOI 10.1137/S1064827502412887. MR2047204

[22] C. R. Dohrmann, *An approximate BDDC preconditioner*, Numer. Linear Algebra Appl. **14** (2007), no. 2, 149–168, DOI 10.1002/nla.514. MR2292301

[23] C. R. Dohrmann and C. Pechstein, *Constraint and weight selection algorithms for BDDC*, Slides for a talk by Dohrmann at DD21 in Rennes, France, June 2012. URL=http://www.numa.uni-linz.ac.at/ clemens/dohrmann-pechstein-dd21-talk.pdf.

[24] C. R. Dohrmann and O. B. Widlund, *An iterative substructuring algorithm for two-dimensional problems in H(curl)*, SIAM J. Numer. Anal. **50** (2012), no. 3, 1004–1028, DOI 10.1137/100818145. MR2970732

[25] C. R. Dohrmann and O. B. Widlund, *Some recent tools and a BDDC algorithm for 3D problems in H(curl)*, Domain decomposition methods in science and engineering XX, Lect. Notes Comput. Sci. Eng., vol. 91, Springer, Heidelberg, 2013, pp. 15–25. MR3242973

[26] C. R. Dohrmann and O. B. Widlund, *A BDDC algorithm with deluxe scaling for three-dimensional H(**curl**) problems*, Comm. Pure Appl. Math. **69** (2016), no. 4, 745–770, DOI 10.1002/cpa.21574. MR3465088

[27] M. Dryja, J. Galvis, and M. Sarkis, *BDDC methods for discontinuous Galerkin discretization of elliptic problems*, J. Complexity **23** (2007), no. 4-6, 715–739, DOI 10.1016/j.jco.2007.02.003. MR2372024

[28] M. Dryja and O. B. Widlund, *Schwarz methods of Neumann-Neumann type for three-dimensional elliptic finite element problems*, Comm. Pure Appl. Math. **48** (1995), no. 2, 121–155, DOI 10.1002/cpa.3160480203. MR1319698

[29] C. Farhat, M. Lesoinne, P. LeTallec, K. Pierson, and D. Rixen, *FETI-DP: a dual-primal unified FETI method. I. A faster alternative to the two-level FETI method*, Internat. J. Numer. Methods Engrg. **50** (2001), no. 7, 1523–1544, DOI 10.1002/nme.76. MR1813746

[30] C. Farhat, J. Mandel, and F.-X. Roux, *Optimal convergence properties of the FETI domain decomposition method*, Comput. Methods Appl. Mech. Engrg. **115** (1994), no. 3-4, 365–385, DOI 10.1016/0045-7825(94)90068-X. MR1285024

[31] C. Farhat and F.-X. Roux, *A method of finite element tearing and interconnecting its parallel solution algorithm*, Internat. J. Numer. Methods Engrg. **32** (1991), 1205–1227. MR1813746

[32] Y. Fragakis and M. Papadrakakis, *The mosaic of high performance domain decomposition methods for structural mechanics: Formulation, interrelation and numerical efficiency of primal and dual methods*, Comput. Methods Appl. Mech. Engrg **192** (2003), 3799–3830.

[33] R. Hiptmair and A. Toselli, *Overlapping and multilevel Schwarz methods for vector valued elliptic problems in three dimensions*, Parallel Solution of Partial Differential Equations (Minneapolis, MN, 1997), IMA Vol. Math. Appl., vol. 120, Springer, New York, 2000, pp. 181–208, DOI 10.1007/978-1-4612-1176-1_8. MR1838270

[34] R. Hiptmair, G. Widmer, and J. Zou, *Auxiliary space preconditioning in H_0(curl; Ω)*, Numer. Math. **103** (2006), no. 3, 435–459, DOI 10.1007/s00211-006-0683-0. MR2221057

[35] R. Hiptmair and J. Xu, *Nodal auxiliary space preconditioning in $\mathbf{H}$(**curl**) and $\mathbf{H}$(div) spaces*, SIAM J. Numer. Anal. **45** (2007), no. 6, 2483–2509, DOI 10.1137/060660588. MR2361899

[36] R. Hiptmair, *Multigrid method for Maxwell's equations*, SIAM J. Numer. Anal. **36** (1999), no. 1, 204–225, DOI 10.1137/S0036142997326203. MR1654571

[37] G. Karypis, *METIS and ParMETIS*, Encyclopedia of Parallel Computing (David Padua, ed.), Springer US, 2011, pp. 1117–1124 (English).

[38] H. H. Kim and E. T. Chung, *A BDDC algorithm with enriched coarse spaces for two-dimensional elliptic problems with oscillatory and high contrast coefficients*, Multiscale Model. Simul. **13** (2015), no. 2, 571–593, DOI 10.1137/140970598. MR3350292

[39] H. H. Kim, E. T. Chung, and J. Wang, *BDDC and FETI-DP algorithms with adaptive coarse spaces for three-dimensional elliptic problems with oscillatory and high contrast coefficients*, http://arxiv.org/abs/1606.07560, August 2015.

[40] A. Klawonn, P. Radtke, and O. Rheinbach, *A comparison of adaptive coarse spaces for iterative substructuring in two dimensions*, Electron. Trans. Numer. Anal. **45** (2016), 75–106. MR3480118

[41] A. Klawonn and O. Rheinbach, *Robust FETI-DP methods for heterogeneous three dimensional elasticity problems*, Comput. Methods Appl. Mech. Engrg. **196** (2007), no. 8, 1400–1414, DOI 10.1016/j.cma.2006.03.023. MR2277025

[42] A. Klawonn, O. Rheinbach, and O. B. Widlund, *An analysis of a FETI-DP algorithm on irregular subdomains in the plane*, SIAM J. Numer. Anal. **46** (2008), no. 5, 2484–2504, DOI 10.1137/070688675. MR2421044

[43] A. Klawonn, O. B. Widlund, and M. Dryja, *Dual-primal FETI methods for three-dimensional elliptic problems with heterogeneous coefficients*, SIAM J. Numer. Anal. **40** (2002), no. 1, 159–179, DOI 10.1137/S0036142901388081. MR1921914

[44] T. V. Kolev and P. S. Vassilevski, *Parallel auxiliary space AMG solver for $H(\mathrm{div})$ problems*, SIAM J. Sci. Comput. **34** (2012), no. 6, A3079–A3098, DOI 10.1137/110859361. MR3029843

[45] J. Kraus, R. Lazarov, M. Lymbery, S. Margenov, and L. Zikatanov, *Preconditioning heterogeneous $H(\mathrm{div})$ problems by additive Schur complement approximation and applications*, SIAM J. Sci. Comput. **38** (2016), no. 2, A875–A898, DOI 10.1137/140974092. MR3474851

[46] P. Le Tallec, *Domain decomposition methods in computational mechanics*, Comput. Mech. Adv. **1** (1994), no. 2, 121–220. MR1263805

[47] J. H. Lee, *A balancing domain decomposition by constraints deluxe method for Reissner-Mindlin plates with Falk-Tu elements*, SIAM J. Numer. Anal. **53** (2015), no. 1, 63–81, DOI 10.1137/130940669. MR3296615

[48] J. Li and X. Tu, *Convergence analysis of a balancing domain decomposition method for solving a class of indefinite linear systems*, Numer. Linear Algebra Appl. **16** (2009), no. 9, 745–773, DOI 10.1002/nla.639. MR2554500

[49] J. Li and O. Widlund, *BDDC algorithms for incompressible Stokes equations*, SIAM J. Numer. Anal. **44** (2006), no. 6, 2432–2455, DOI 10.1137/050628556. MR2272601

[50] J. Li and O. B. Widlund, *FETI-DP, BDDC, and block Cholesky methods*, Internat. J. Numer. Methods Engrg. **66** (2006), no. 2, 250–271, DOI 10.1002/nme.1553. MR2224479

[51] P. Lin, *A sequential regularization method for time-dependent incompressible Navier-Stokes equations*, SIAM J. Numer. Anal. **34** (1997), no. 3, 1051–1071, DOI 10.1137/S0036142994270521. MR1451113

[52] A. Logg, K.-A. Mardal, and G. N. Wells (eds.), *Automated Solution of Differential Equations by the Finite Element Method*, Lecture Notes in Computational Science and Engineering, vol. 84, Springer, Heidelberg, 2012. The FEniCS book. MR3075806

[53] A. Logg and G. N. Wells, *DOLFIN: automated finite element computing*, ACM Trans. Math. Software **37** (2010), no. 2, Art. 20, 28, DOI 10.1145/1731022.1731030. MR2738227

[54] J. Mandel and M. Brezina, *Balancing domain decomposition for problems with large jumps in coefficients*, Math. Comp. **65** (1996), no. 216, 1387–1401, DOI 10.1090/S0025-5718-96-00757-0. MR1351204

[55] J. Mandel and C. R. Dohrmann, *Convergence of a balancing domain decomposition by constraints and energy minimization*, Numer. Linear Algebra Appl. **10** (2003), no. 7, 639–659, DOI 10.1002/nla.341. Dedicated to the 70th birthday of Ivo Marek. MR2030628

[56] J. Mandel, C. R. Dohrmann, and R. Tezaur, *An algebraic theory for primal and dual substructuring methods by constraints*, Appl. Numer. Math. **54** (2005), no. 2, 167–193, DOI 10.1016/j.apnum.2004.09.022. MR2148040

[57] J. Mandel and B. Sousedík, *Adaptive selection of face coarse degrees of freedom in the BDDC and the FETI-DP iterative substructuring methods*, Comput. Methods Appl. Mech. Engrg. **196** (2007), no. 8, 1389–1399, DOI 10.1016/j.cma.2006.03.010. MR2277024

[58] J. Mandel, B. Sousedík, and J. Šístek, *Adaptive BDDC in three dimensions*, Math. Comput. Simulation **82** (2012), no. 10, 1812–1831, DOI 10.1016/j.matcom.2011.03.014. MR2967935

[59] J. Mandel and R. Tezaur, *On the convergence of a dual-primal substructuring method*, Numer. Math. **88** (2001), no. 3, 543–558, DOI 10.1007/s211-001-8014-1. MR1835470

[60] P. Monk, *Finite Element Methods for Maxwell's Equations*, Numerical Mathematics and Scientific Computation, Oxford University Press, New York, 2003. MR2059447

[61] J.-C. Nédélec, *Mixed finite elements in $\mathbf{R}^3$*, Numer. Math. **35** (1980), no. 3, 315–341, DOI 10.1007/BF01396415. MR592160

[62] D.-S. Oh, *Domain Decomposition Methods for Raviart-Thomas Vector Fields*, ProQuest LLC, Ann Arbor, MI, 2011. Thesis (Ph.D.)–New York University. MR2982343

[63] D.-S. Oh, *An overlapping Schwarz algorithm for Raviart-Thomas vector fields with discontinuous coefficients*, SIAM J. Numer. Anal. **51** (2013), no. 1, 297–321, DOI 10.1137/110838868. MR3033012

[64] D.-S. Oh, *A BDDC Preconditioner for Problems Posed in $H(\mathrm{div})$ with Deluxe Scaling*, Domain decomposition methods in science and engineering XXII, Lect. Notes Comput. Sci. Eng., vol. 104, Springer, Heidelberg, 2016, pp. 355–361.

[65] L. F. Pavarino, *BDDC and FETI-DP preconditioners for spectral element discretizations*, Comput. Methods Appl. Mech. Engrg. **196** (2007), no. 8, 1380–1388, DOI 10.1016/j.cma.2006.03.009. MR2277023

[66] L. F. Pavarino, O. B. Widlund, and S. Zampini, *BDDC preconditioners for spectral element discretizations of almost incompressible elasticity in three dimensions*, SIAM J. Sci. Comput. **32** (2010), no. 6, 3604–3626, DOI 10.1137/100791701. MR2763740

[67] C. Pechstein and C. R. Dohrmann, *Modern domain decomposition methods, BDDC, deluxe scaling, and an algebraic approach.*, Talk by Pechstein in Linz, Austria. URL: http://people.ricam.oeaw.ac.at/c.pechstein/pechstein-bddc2013.pdf, 2013.

[68] C. Pechstein and C. R. Dohrmann, *A Unified Framework for Adaptive BDDC*, Tech. Report 2016-20, Johann Radon Institute for Computational and Applied Mathematics (RICAM), 2016, URL:http://www.ricam.oeaw.ac.at/files/reports/16/rep16-20.pdf.

[69] A. Quarteroni and A. Valli, *Numerical Approximation of Partial Differential Equations*, Springer Series in Computational Mathematics, vol. 23, Springer-Verlag, Berlin, 1994. MR1299729

[70] B. Sousedík, *Nested BDDC for a saddle-point problem*, Numer. Math. **125** (2013), no. 4, 761–783, DOI 10.1007/s00211-013-0548-2. MR3127330

[71] A. Toselli, *Neumann-Neumann methods for vector field problems*, Electron. Trans. Numer. Anal. **11** (2000), 1–24. MR1749071

[72] A. Toselli, *Overlapping Schwarz methods for Maxwell's equations in three dimensions*, Numer. Math. **86** (2000), no. 4, 733–752, DOI 10.1007/PL00005417. MR1794350

[73] A. Toselli, *Dual-primal FETI algorithms for edge finite-element approximations in 3D*, IMA J. Numer. Anal. **26** (2006), no. 1, 96–130, DOI 10.1093/imanum/dri023. MR2193972

[74] A. Toselli and A. Klawonn, *A FETI domain decomposition method for edge element approximations in two dimensions with discontinuous coefficients*, SIAM J. Numer. Anal. **39** (2001), no. 3, 932–956, DOI 10.1137/S0036142999361372. MR1860451

[75] A. Toselli and O. Widlund, *Domain Decomposition Methods—Algorithms and Theory*, Springer Series in Computational Mathematics, vol. 34, Springer-Verlag, Berlin, 2005. MR2104179

[76] X. Tu, *A BDDC algorithm for a mixed formulation of flow in porous media*, Electron. Trans. Numer. Anal. **20** (2005), 164–179. MR2175341

[77] X. Tu, *A BDDC algorithm for flow in porous media with a hybrid finite element discretization*, Electron. Trans. Numer. Anal. **26** (2007), 146–160. MR2366094

[78] X. Tu, *Three-level BDDC in three dimensions*, SIAM J. Sci. Comput. **29** (2007), no. 4, 1759–1780, DOI 10.1137/050629902. MR2341811

[79] X. Tu, *Three-level BDDC in two dimensions*, Internat. J. Numer. Methods Engrg. **69** (2007), no. 1, 33–59, DOI 10.1002/nme.1753. MR2282536

[80] X. Tu, *A three-level BDDC algorithm for a saddle point problem*, Numer. Math. **119** (2011), no. 1, 189–217, DOI 10.1007/s00211-011-0375-2. MR2824859

[81] X. Tu and J. Li, *A balancing domain decomposition method by constraints for advection-diffusion problems*, Commun. Appl. Math. Comput. Sci. **3** (2008), 25–60, DOI 10.2140/camcos.2008.3.25. MR2425545

[82] P. S. Vassilevski and U. Villa, *A mixed formulation for the Brinkman problem*, SIAM J. Numer. Anal. **52** (2014), no. 1, 258–281, DOI 10.1137/120884109. MR3162407

[83] O. B. Widlund and C. R. Dohrmann, *BDDC Deluxe Domain Decomposition*, Domain decomposition methods in science and engineering XXII, Lect. Notes Comput. Sci. Eng., vol. 104, Springer, Heidelberg, 2016, pp. 93–103.

[84] B. I. Wohlmuth, *Discretization Methods and Iterative Solvers Based on Domain Decomposition*, Lecture Notes in Computational Science and Engineering, vol. 17, Springer-Verlag, Berlin, 2001. MR1820470

[85] B. I. Wohlmuth, A. Toselli, and O. B. Widlund, *An iterative substructuring method for Raviart-Thomas vector fields in three dimensions*, SIAM J. Numer. Anal. **37** (2000), no. 5, 1657–1676, DOI 10.1137/S0036142998347310. MR1759911

[86] S. Zampini and D. E. Keyes, *On the Robustness and Prospects of Adaptive BDDC Methods for Finite Element Discretizations of Elliptic PDES with High-contrast Coefficients*, Proceedings of the Platform for Advanced Scientific Computing Conference (New York, NY, USA), PASC '16, ACM, 2016, pp. 6:1–6:13.

[87] S. Zampini, *Dual-primal methods for the cardiac bidomain model*, Math. Models Methods Appl. Sci. **24** (2014), no. 4, 667–696. MR3163396

[88] S. Zampini, *Adaptive BDDC Deluxe Methods for H(curl)*, Proceedings of the 23rd International Conference on Domain Decomposition Methods, Lecture Notes in Computational Science and Engineering, vol. 116, Springer, 2017, pp. 285–292.

[89] S. Zampini, *PCBDDC: a class of robust dual-primal methods in PETSc*, SIAM J. Sci. Comput. **38** (2016), no. 5, S282–S306, DOI 10.1137/15M1025785. MR3565564

[90] S. Zampini and X. Tu, *Adaptive Multilevel BDDC Deluxe Algorithms for Flow in Porous Media*, Tech. report, 2016, submitted.

Department of Mathematics, Rutgers University, Piscataway, New Jersey 08854
E-mail address: duksoon@math.rutgers.edu

Courant Institute of Mathematical Sciences, 251 Mercer Street, New York, New York 10012
E-mail address: widlund@cims.nyu.edu

Computer, Electrical and Mathematical Sciences and Engineering Division, Extreme Computing Research Center, King Abdullah University of Science and Technology, Thuwal 23955-6900, Saudi Arabia
E-mail address: stefano.zampini@kaust.edu.sa

Computational Solid Mechanics and Structural Dynamics, Sandia National Laboratories, Albuquerque, New Mexico, 87185
E-mail address: crdohrm@sandia.gov